Nasopharyngeal carcinoma: past, present and future directions

by

Zahra Taheri-Kadkhoda

Department of Oncology
Institute of Clinical Sciences
Göteborg University
SWEDEN

2007

GÖTEBORG UNIVERSITY

ABSTRACT

Nasopharyngeal carcinoma: past, present and future directions

Zahra Taheri-Kadkhoda, Department of Oncology, Institute of Clinical Sciences,
Göteborg University, S-413 45 Göteborg, Sweden.

Nasopharyngeal carcinoma (NPC) is a rare disease in Sweden. The purpose of this thesis was to investigate the clinicopathological manifestations of the disease and its treatment outcomes in a cohort of Swedish NPC patients to identify key features for future improvements in patient care.

From 1991 to 2002, 50 NPC patients were treated with radical three-dimensional conformal radiotherapy (3DCRT) +/- intracavitary brachytherapy (IBT) +/- chemotherapy at Jubileumskliniken, Sahlgrenska University Hospital. Retrospective analysis of the data showed 5-year local, regional, and distant relapse-free survival rates of 70%, 92%, and 77% for 49 nondisseminated patients. Patients with locoregionally advanced disease fared worse with respect to local and distant tumor control rates. Furthermore, the long-term side effects of irradiation were adverse and frequent in the whole cohort of patients.

A comparative treatment planning study between intensity-modulated radiotherapy (IMRT) and 3DCRT + IBT was performed for eight NPC patients. The prescription physical dose for planning target volume of the primary tumor was 72.6 Gy in IMRT and 72 Gy in the combined plans. The comparison of the plans using quantitative parameters revealed that IMRT plans provided more conformal plans with possibility of dose escalation in primary tumor and simultaneous sparing of several normal structures. These were translated into improved tumor control probability of the primary tumor and reduction of normal tissue complication probability for several organs. However IMRT plans resulted in significant increase of the mean volumes of low to intermediate isodoses (0.66 Gy to 19.8 Gy) by 30% to 44%.

A comparative treatment planning study between IMRT and intensity-modulated proton therapy (IMPT) with equivalent dose prescriptions for primary tumour (72.6 Gy_E) in the same cohort of patients showed that conformity of treatment plans and tumor coverage especially for locally advanced tumors were improved further by IMPT plans. Moreover, the integral dose (mean dose) was significantly reduced by a factor of 2 to 3 in several organs. The mean volume of low to intermediate isodoses (0.66 Gy to 19.8 Gy) were 2 to 2.7-fold larger in IMRT plans than in IMPT plans.

Expression of EBV-encoded LMP1, Ki-67, cyclin-B1, and EGFR were analyzed by immunohistochemical assays for 44 (45 for LMP1) NPC patients. LMP1 was expressed in 33% of the patients and its presence was significantly correlated with advanced nodal and tumour stage. Statistically, expression of Ki-67 and cyclin-B1 showed no significant clinical relevance. Strong EGFR staining intensity was significantly correlated with worse 5-year local and locoregional tumor control probabilities as well as poorer disease-free and overall survival rates.

Key words: Nasopharyngeal carcinoma, radiotherapy, side effects, 3DCRT, Intracavitary brachytherapy, IMRT, IMPT, LMP1, EGFR.
ISBN: 978-91-628-7323-3

Share your knowledge,

it is a way to achieve immortality!

Dalai Lama

To my beloved parents

sister and brothers

LIST OF PUBLICATIONS

This thesis is based on the following papers, which will be referred to in the text by their Roman numerals:

I Taheri-Kadkhoda Z, Björk-Eriksson T, Johansson K-A, and Mercke C. Long-term treatment results for nasopharyngeal carcinoma: The Sahlgrenska University Hospital experience. *Acta Oncol. 2007;46(6):817-827.*

II Taheri-Kadkhoda Z, Pettersson N, Björk-Eriksson T, and Johansson K-A. Superiority of intensity-modulated radiotherapy over three-dimensional conformal radiotherapy combined with brachytherapy in nasopharyngeal carcinoma: a planning study. *Accepted by The British Journal of Radiology on August 14th,2007.*

III Taheri-Kadkhoda Z, Björk-Eriksson T, Nill S, Wilkens JJ, Oelfke U, Johansson K-A, Huber PE, and Műnter MW. Intensity-modulated radiotherapy of nasopharyngeal carcinoma: a comparative treatment planning study of photons and protons. *Submitted.*

IV Taheri-Kadkhoda Z, Magnusson B, Svensson M, Mercke C, and Björk-Eriksson T. Expression modes and clinical manifestations of LMP1, Ki-67, cyclin-B1, and epidermal growth factor receptor in non-endemic nasopharyngeal carcinoma. *In manuscript.*

CONTENTS

page

ABBREVIATIONS

2DRT	Two-dimensional radiotherapy
3DCRT	Three-dimensional conformal radiotherapy
AJCC	American joint committee on cancer
CHT	Chemotherapy
CI	Conformity index
CRT	Conventional radiotherapy
CT	Computed tomography
CTCAE	Common terminology criteria for adverse events
CTV	Clinical target volume
Cyclin-B1	Phase specific protein of the cell cycle expressed in G2 + M phase
DFS	Disease-free survival
DRFS	Distant relapse-free survival
DVH	Dose volume histogram
EBV	Epstein-Barr virus
EGFR	Epidermal growth factor receptor
EQD2	Equivalent dose in 2 Gy fractions
EUD	Equivalent uniform dose
GTV	Gross tumour volume
H & N	Head and neck
HART	Hyperfractionated accelerated radiotherapy
HDR	High dose rate
IBT	Intracavitary brachytherapy
IC	Inhomogeneity coefficient
ICRU	International commission on radiation units and measurements
IHC	Immunohistochemistry
IMPT	Intensity-modulated proton therapy
IMRT	Intensity-modulated radiotherapy
JK	Jubileumskliniken
Ki-67	Nuclear antigen expressed only by proliferating cells

LDR	Low dose rate
LENT/SOMA	Late effects of radiotherapy in normal tissues/subjective, objective, management, and analytical scoring system
LET	Linear energy transfer
LKB model	Lyman-Kutcher-Burman model
LMP1	Latent membrane protein 1 encoded by Epstein-Barr virus
LRFS	Local relapse-free survival
LRRFS	Locoregional relapse-free survival
MLC	Multi-leaf collimator
MLI	Mean luminescence intensity
MRI	Magnetic resonance imaging
NPC	Nasopharyngeal carcinoma
NTCP	Normal tissue complication probability
OAR	Organs at risk
OC	Oncology Center
OS	Overall survival
OTT	Overall treatment time
PFS	Progression-free survival
PET	Positron emission tomography
PTV	Planning target volume
RBE	Relative biological effectiveness
RT	Radiotherapy
SCC	Squamous cell carcinoma
SF	Surviving fraction
SIB	Simultaneous integrated boost
SOBP	Spread out bragg peak
TCP	Tumour control probability
TM	Temporomandibular
UICC	International union against cancer
WHO	World health organization

AIMS OF THE STUDY

The aims of the studies included in this thesis are as follows;

- To assess whether the traditional treatment strategies for nasopharyngeal carcinoma (NPC) patients in our institution have resulted in satisfactory survival outcomes and acceptable side-effect profiles and to identify key features for future improvements (Paper I).

- To assess whether currently available intensity-modulated radiotherapy technique has the potential to provide better clinical outcomes for NPC patients than conventional radiotherapy techniques (Paper II).

- To assess whether proton therapy can potentially be beneficial for primary treatment of NPC patients in future (Paper III).

- To assess whether there are biomarkers with prognostic and therapeutic values in nonendemic NPC (Paper IV).

INTRODUCTION

Nasopharyngeal carcinoma (NPC) occurs worldwide, yet its incidence and histopathological presentations show broad geographical variations. Radiotherapy (RT) is the main therapeutic modality in primary treatment of NPC and the chance of cure is highly dependent on tumour stage and the delivered dose. The nasopharyngeal cavity is surrounded by several dose-limiting normal tissues that impede delivery of an adequate dose or sufficient coverage of the locally advanced tumours when conventional RT techniques are used. Moreover, the inevitable inclusion of normal structures in the trajectory of the beams used in RT of NPC and the delivery of doses above their tolerance threshold are frequently associated with a higher risk of permanent dysfunction of these structures. Consequently, the results of RT alone, in locoregionally advanced NPC, have been somewhat discouraging with respect to local and distant tumour control, and the side effects of such treatment have often been adverse and chronic for the whole group (1). In the past decades, much effort has focused on improving the clinical outcomes in NPC patients. The potential of modern RT techniques to increase tumour control and reduce RT-related side effects has been evaluated in small clinical studies (2, 3), and a combined treatment strategy including chemoradiotherapy is currently recommended for locoregionally advanced NPC in order to improve tumour control and survival (4, 5). Most of our knowledge of NPC from the molecular to the clinical level is based on the experience from areas of the world with a high incidence of the tumour, the so-called endemic regions. Although very valuable, these informations may not always apply to NPC patients from nonendemic regions such as Sweden because of etiological and histological differences.

In this thesis, I have chosen to investigate the molecular and clinical manifestations and treatment outcomes in NPC patients from a nonendemic region in order to identify key features for future improvements in patient care. A major part of the research is also devoted to evaluating new RT techniques in NPC, with results that may have global impact.

BACKGROUND

Epidemiology and Aetiology

Nasopharyngeal carcinoma is an endemic disease of Southeast Asia with incidence rates of between 15 and 50 per 100 000 (6). There is an intermediate incidence in North Africa and far northern hemisphere. In the West, the disease occurs sporadically and in Sweden the incidence

rate is very low, varying between 0.3 and 0.4 per 100 000 (7). In this country, NPC constitutes only 0.1% of all new cancer cases each year (7). Globally, NPC shows a bimodal age distribution. A small peak is observed in late childhood and a second peak occurs in people aged 50-60 years (8). The disease is more common in males than females by a ratio of 2-3:1 (1, 9, 10).

Unlike other squamous cell cancers (SCCs) of the head and neck (H & N) region, NPC does not appear to be linked to excessive use of tobacco and alcohol. The proposed predisposing factors include diet, viral agents such as Epstein-Barr virus (EBV), and genetic susceptibility (6). It has been suggested that chronic exposure to volatile nitrosamines released during the cooking of salted food items such as fish may irritate the nasopharyngeal mucosa. This irritation, with or without genetic predispositions can lead to development of patchy low-grade dysplasias in the nasopharyngeal mucosa. At this stage, latent EBV infection may aggravate the dysplatic status of the mucosa and together with further chromosomal aberrations may result in the development of invasive cancer. The metastatic behaviour of the tumour is associated with p53 mutation and aberrant expression of cadherins (6). Figure 1. demonstrates a proposed carcinogenesis model for NPC.

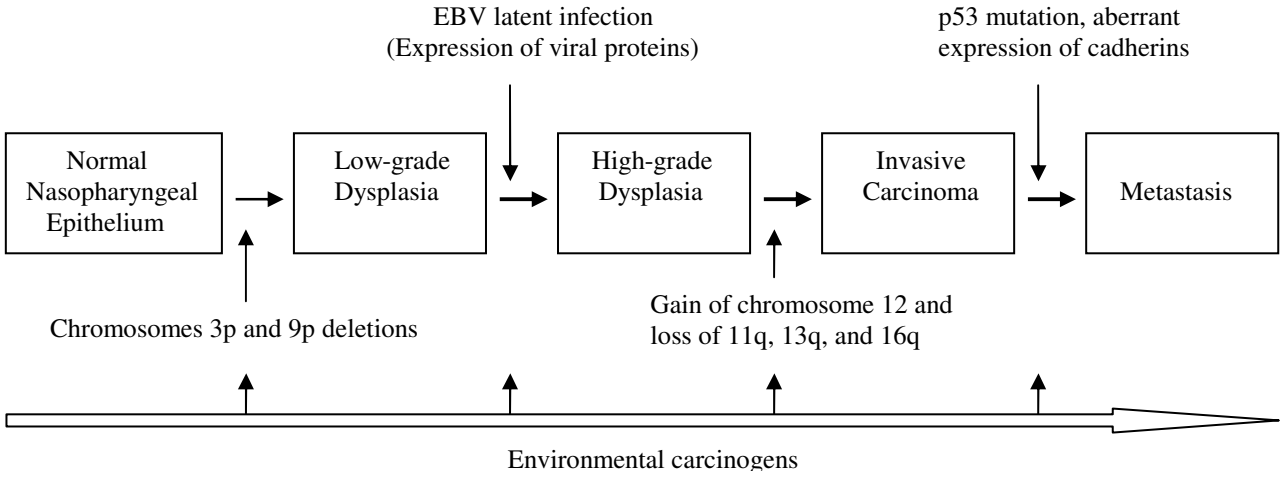

Figure 1. A proposed carcinogenesis pathway for nasopharyngeal carcinoma (6).

Anatomy

The nasopharyngeal cavity is a cuboidal structure covered by stratified mucociliary columnar epithelium (Figure 2). The superior and posterior borders are formed by the bony structures of the basiocciput, basisphenoid, and the first two cervical vertebrae. The inferior and anterior

boundaries are upper surface of the soft palate and the posterior choanae, respectively. The lateral walls contain the Eustachian tube openings (torus tubarii) behind which is the lateral pharyngeal recess (fossa Rosenmuller), the most common site for development of NPC.

Figure 2. Anatomy of nasopharyngeal cavity.

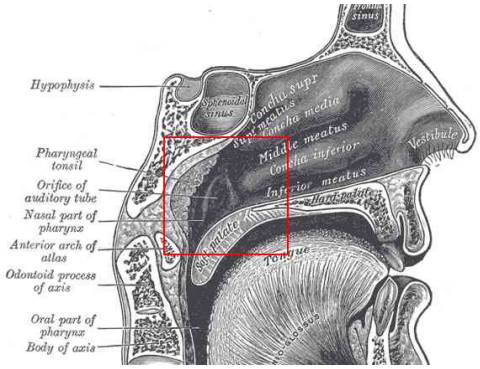

The anatomical localization of the nasopharyngeal cavity has important clinical implications. Any tumour originating in this region can expand and infiltrate several normal structures that surround the cavity. These structures include neural structures, the auditory apparatus, masticatory muscles, the temporomandibular (TM) joints, and the parotid glands. Moreover, these structures can be at risk of damage depending on the treatment modality that is chosen to reach and cure the tumour in the nasopharynx. Figures 3. shows magnetic resonance images (MRIs) from three NPC patients with several normal structures surrounding the tumours.

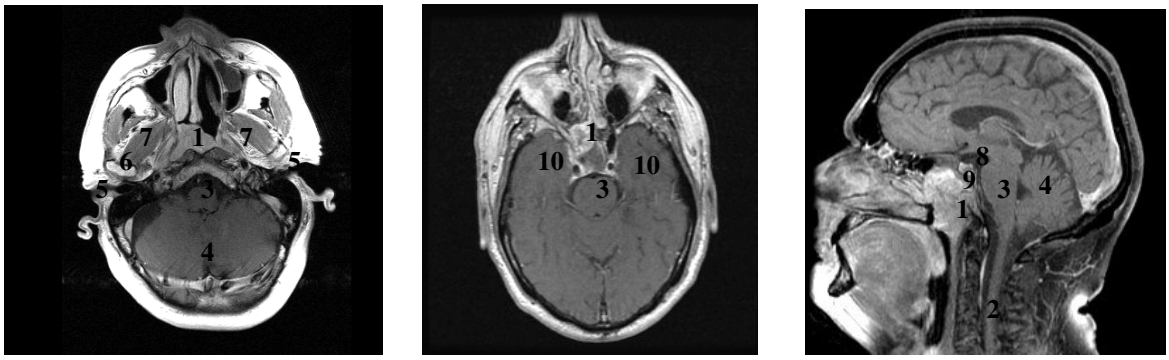

Figure 3. MRI of a nasopharyngeal carcinoma and neighbouring normal structures in three NPC patients treated at Jubileumskliniken, Sahlgrenska University Hospital. (1. Tumour, 2. Spinal cord, 3. Brainstem, 4. Cerebellum, 5. Auditory channal, 6. Temporomandibular joint, 7. External pterygoid muscle, 8. Optic chiasm, 9. Pituitary gland, 10. Temporal lobe).

Histopathology

The World Health Organization (WHO) has recognized three histopathological types for the epithelial neoplasms of the nasophoryngeal cavity (11). These types are keratinizing SCC (WHO type I), nonkeratinizing carcinoma (WHO type II) including transitional and intermediate cell carcinoma, and the undifferentiated carcinoma (WHO type III) including anaplastic and clear cell carcinoma. The term lymphoepithelial carcinoma is used for both WHO types II and III when cancer cells are mixed with lymphoid stroma. In that case, the two groups are also referred as Regaud and Schminke tumours, respectively. The WHO type III most frequently presents at diagnosis especially in the endemic regions. While WHO type I is scarce in endemic regions, it is relatively more frequent in nonendemic areas. In North America the distribution of WHO types I, II, and III in NPC patients is 25%, 12%, and 63%, respectively. The corresponding figures in patients from southern China are 2%, 3%, and 95% (12). WHO type II and III tumours are frequently associated with latent EBV infection in 86% to nearly 100% of the patients (13, 14).

Natural History

Nasopharyngeal carcinoma can grow by expansion into the nasal cavity, oro-, and hypopharynx. Additionally, through infiltration of the pharyngobasilar fascia, the tumour can invade the soft tissues and bony structures surrounding the nasopharyngeal cavity. The tumour can also gain entry into the intracranial cavity through foramina in the base of skull with cranial nerve encroachment as a consequence. The nasopharyngeal cavity is served by abundant lymphatic drainage. Cancers arising in this location have a propensity for metastasis to lymph nodes along the retropharyngeal, accessory nerve, and jugular vein pathways. Accordingly, cervical mass is the most common presenting symptom in NPC, occuring in up to 90% of patients (15). Other presenting symptoms and signs in NPC patients include unilateral otitis media or hearing impairment, tinnitus, trismus, nasal obstruction and bleeding, pain, and cranial nerve palsies (12, 15). The metastatic potential of NPC is partly related to its histopathological classification. WHO type I tumours are more likely to show uncontrolled local growth whereas WHO type II-III tumours are frequently associated with cervical nodal metastasis ranging from 80% to 90% (15). Hematogenous spreading is more common in NPC than for other H & N cancers and is predominantly observed in the skeleton, lung, and liver. Distant metastasis can be presented in 5%-11% of the patients at the initial work-up, with the

highest risk for patients with bulky and fixed lymph nodes, bilateral cervical or lower neck disease (15).

Diagnosis

The diagnosis of NPC is established by clinical examination and histological confirmation. The latter is performed by taking biopsies from the nasopharyngeal mass, which is best visualized using a fibreoptic nasopharyngoscope. If a cervical mass presents, fine needle aspirations or extirpation of the node is needed for diagnosis. In order to detect the local and regional extension of the tumour accurately, both a computed tomography (CT) scan and an MRI of the nasopharynx, base of the skull, and neck are recommended. MRI is more sensitive than CT scans for detection of the primary tumour, its parapharyngeal and/or intracranial extension, and bone marrow infiltration (12). However, bony erosions are better detected by CT scans. The role of positron emission tomography (PET) scanning in NPC is still unsettled, although there are indications for using PET in detecting local failures after therapy or distant metastasis(12). Chest X-rays are routinely used for detecting pulmonary metastasis. Radiographic screening of other sites of the body including the abdomen and skeleton is usually done when the results of clinical and laboratory work-up of the patient suggest distant metastasis (12, 16).

Classification and prognostic factors

Several systems for NPC stage classification have been developed. The Ho classification (17) has been widely used in Asia. This system differs from most staging systems in that it comprises three T stages and five overall stages. In 1997, the International Union Against Cancer (UICC) and the American Joint Committee on Cancer (AJCC) jointly formulated a new stage classification for NPC. This classification incorporates major tumour parameters that are prognostically significant (Table 1) (18, 19).

Major prognostic factors adversely influencing the outcome of treatment in NPC patients include tumour size, disease extent as measured by staging systems, and the type of histology (6). Based on the difference in failure patterns, four prognostic categories can be defined across the NPC stages. These are; T1-T2N0-N1 tumours with relatively good treatment outcome; T3-T4N0-N1 tumours with mainly local failure; T1-T2N2-N3 with mainly regional and distant failure; and T3-T4N2-N3 with local, regional, and distant failure.

Table 1. Staging criteria for nasopharyngeal carcinoma according to UICC/AJCC 1997 system (18, 19).

Nasopharynx (T)	
T1	Nasopharynx
T2	Soft tissue of oropharynx and/or nasal fossa
T2a	Without parapharyngeal extension
T2b	With parapharyngeal extension
T3	Invasion of bony structure and/or paranasal sinuses
T4	Intracranial extension, involvement of cranial nerves, infratemporal fossa, hypopharynx, orbit
Regional lymph node (N)	
N1	Unilateral metastasis in lymph node(s), ≤6 cm in greatest dimension, above supraclavicular fossa
N2	Bilateral metastasis in lymph node(s), ≤6 cm in greatest dimension, above supraclavicular fossa
N3	Metastasis in lymph node(s), >6 cm in dimension, in the supraclavicular fossa
Distant metastasis (M)	
M0	No distant metastasis
M1	Distant metastasis
Stage grouping	
Stage 0	Tis N0 M0
Stage I	T1 N0 M0
Stage IIa	T2a N0 M0
Stage IIb	T2b N0 M0, T1-T2 N1 M0
Stage III	T3 N0-N3 M0, T1-T2 N2 M0
Stage IVa	T4 N0-N2 M0
Stage IVb	Any T N3 M0
Stage IVc	Any T Any N M1

Histopathologically, WHO type III tumours are associated with a better prognosis showing 5-year OS rate of 60% depending on the tumour stage, compared with an OS rate as low as 15% in WHO type I tumours (15). Other factors linked to tumour control and survival rates that were present in some, but not all, studies include age, the total RT dose, latent EBV infection, and overexpression of biomarkers such as epidermal growth factor receptor (EGFR) in the tumour specimens (1, 14, 20, 21). In some studies, the presence of latent membrane protein 1 (LMP1), an EBV-encoded oncoprotein, and increased expression of the proliferation marker Ki-67 in NPC patients have been correlated to advanced nodal and tumour stage (22, 23). Among phase specific proteins of the cell cycle (cyclins), the prognostic value of cyclin-B1 expression has been on focus in recent years. Although it has been demonstrated that overexpression of this molecule in H & N cancers is correlated to poorer tumour control rates (24, 25), there are no reports on patterns of expression or clinical manifestations of this marker in NPC patients.

Treatment

Surgery

Due to the location of the primary tumour in NPC and the faint chances of achieving clean resection margins, surgery is usually not feasible in primary treatment of the lesions and is reserved for highly selected patients with residual disease or recurrence of the disease (12). In these cases, 5-year tumour control rate of 65% is reported when tumour is adequately resected (12). However, surgery in the form of nasopharyngectomy is associated with considerable morbidity, including risk of injuries to the cranial nerves, cerebral fluid leaks, and haemorrhage secondary to vessel injury (15). Surgery is also not advocated in primary treatment of cervical lymph node metastases. These metastases are mostly radiosensitive and radiocurable, and are often bulky and bilateral. In addition, those located in the nodes of Rouviere are not accessible for surgery. The risk of isolated regional failure in the neck is less than 5% in NPC patients after combined chemoradiation (12). For those patients where failure occurs, radical neck dissection is recommended, sometimes in combination with brachytherapy.

Chemotherapy

Chemotherapy (CHT) is frequently combined with RT in locoregionally advanced NPC. There are three basic approaches: neoadjuvant, concomitant, or adjuvant treatment. The most common combination of CHT agents used for NPC patients is cisplatin and 5-fluorouracil (5-FU). More than ten randomized trials have been performed to evaluate the benefits of chemoradiotherapy over RT alone in NPC patients (12). The 1997 intergroup study from the nonendemic region was the first to show significant benefits in terms of progression-free (PFS) and OS rates in locoregionally advanced NPC patients who received concomitant and adjuvant CHT plus RT (69% and 76%) compared with those received RT only (24% and 46%) (26). This study has been criticized for the inferior results in the RT arm compared with historical results from the endemic regions. The applicability of results of this study in endemic regions has also been questioned because of the relative high rate of WHO type I presentation in the accrued patients. Two meta-analyses of randomized trials involving NPC patients with locoregionally advanced disease have revealed an absolute 5-year OS benefits of 4% and 6% for chemoradiotherapy (4, 5). In both studies, the benefit was essentially observed when concomitant CHT was administered. While one of these studies (5) demonstrated

significant benefits of both neoadjuvant and concomitant CHT in reduction of locoregional and distant failures, no correlation between the timing of CHT and event-free survival (tumour recurrence or death) rates was found in the other analysis (4). Currently, the standard treatment for locoregionally advanced NPC (stages IIb-IVb) is RT concomitantly with cisplatin. Because of the high risk of distant failure in these patients, protocol-based addition of neoadjuvant CHT is also recommended. For Stages I-IIa NPC tumours, only RT is administered.

Radiotherapy

Radiotherapy involves the use of high-energy photon and/or particle beams (electrons, protons, heavy ion) to ionize molecules and destroy their function in the targeted tissue that they penetrate. This can be done by several approaches but for most clinical purposes such as in NPC, irradiation is done with external radiation sources using high-energy photon and/or electron beams that in modern RT centres are produced and delivered to patients by linear accelerators.

The probability of success rate with RT is highly dependent on the radiosensitivity of the tumour tissue, the delivered dose, and the precision with which it is administered. Radiotherapy is the most important treatment modality in NPC due to its anatomical localization and propensity to bilateral cervical lymph node metastasis. Yet while the eradication of NPC lesions demands high absorbed doses, the ultimate tolerable dose is limited by both acute and late side effects of RT in vital structures surrounding the tumour. Moreover, it is estimated that 70% to 90% of NPC patients have occult and macroscopic cervical lymph node metastasis independent of their T stages (27). Radiotherapy in NPC patients is thus directed to both the primary lesion and the bilateral cervical lymph node stations, including the supraclavicular fossae. Consequently, NPC patients are often treated with large RT beams that inevitably affect normal structures around and below the nasopharyngeal cavity. As a consequence, surviving NPC patients are at higher risk of suffering adverse acute and late side effects of RT than other H & N cancer patients (28).

During the last decades, the accumulation of knowledge in importance of time, dose, and fractionation of RT on tumour response and normal tissue reactions and technical advances in RT have been accompanied by encouraging improvements in 4 to 5-year OS rates of NPC patients from 25% in 1960s to 88% in modern times (2, 9, 29). In the following, a brief description of the technical transitions in irradiation of NPC patients will be presented.

Two-dimensional external radiotherapy

Until the early 1990s, radical external RT for NPC was delivered using two-dimensional RT (2DRT) techniques delivering tumouricidal absorbed doses of 60-70 Gy (2-2.5 Gy/fraction in 6-7 weeks) to anatomical structures with a high suspicion of tumour infiltration (6, 27). A lower dose of 46-50 Gy was delivered to bilateral cervical lymph node stations at risk of tumour invasion (27). This technique involved manual projection of tumour volumes on orthogonal simulation films and employment of nonconformal shielding blocks for critical normal structures. In general, photon beams were used for irradiation, but electron beams were also added when necessary. A typical example of the 2DRT technique for NPC was described by Ho (Figure 4) (30). In the first phase of the treatment, the primary tumour and upper cervical lymph nodes were covered using laterally opposed faciocervical beams and the lower neck was irradiated by an anterior cervical beam. Appropriate shielding was used to protect neural tissues, the oral cavity, and the central structures of the neck including the spinal cord and larynx. When the spinal cord dose reached 40-45 Gy, a second phase of individualized treatment was started. In the treatment planning of the second phase, a shrinking beam technique was used delivering radical doses to the primary tumour and lymph node metastases while sparing major neural tissues from high doses of irradiation. A major objection to this technique was the risk of underdosing the tumour and overdosing normal tissues at the junction between different beams. Furthermore, in the era of 2DRT, definition of the target volumes was based on physical examinations and plain x-ray radiographs. Hence, the likelihood of locoregional tumour control and normal tissue safety relied on the delivered doses, fractions, beam sizes, and their directions without full knowledge of the three-dimensional (3D) distributions of doses and volumes. With radical doses of 2DRT +/- CHT, 5-year local control rates of 78-93% and 53-79% for T1-T2 and T3-T4 tumours have been reported (9, 29, 31). For N0-N1 and N2-N3 diseases, corresponding rates have been 89%-96% and 71%-91% (29, 31). The 5-year OS rates for stages I-II and III-IV have been in order of 50%-90% and 30%-76%, respectively (1, 9, 29, 31). In general, 2DCRT of NPC patients was accompanied by high rate of late side effects such as xerostomia, temporal lobe necrosis, and complications from the auditory apparatus and TM joints (1, 9, 10).

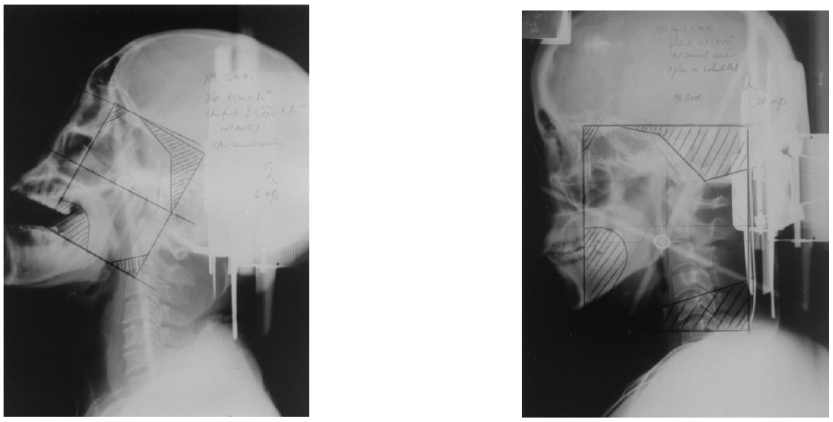

Figure 4. Demonstration of faciocervical beam (right) in the first phase and facial beam (left) in the second phase of Ho irradiation technique for a patient with nasopharyngeal carcinoma (10).

Three-dimensional external radiotherapy

Three-dimensional (3D) treatment planning based on CT scans acquired in the treatment position has been a major breakthrough in RT. Computer tomography of the anatomical regions intended for treatment can provide data for better definition of target and non-target volumes, and accurate estimation of the tissue heterogeneities. Based on these data, number of the beams, their orientations, and shapes can be optimally selected to favor better dose distributions within the target volumes and normal tissues. This is called 3D conformal RT (3DCRT) and its ultimate goal is to increase the tumour control probability (TCP) and decrease the normal tissue complication probability (NTCP) (widening of therapeutic ratio) when irradiating malignant lesions. The principle of 3DCRT is also applied in particle therapy.

According to the recommendations of the International Commission on Radiation Units and measurements, ICRU (32), certain volumes for the tumour and normal tissues must be identified and delineated on the acquired CT slices before the actual treatment planning is performed in 3DCRT. Gross tumour volume (GTV) is the term used for the macroscopic manifestation of the tumour presented as primary lesion and regional lymph node metastasis. Information from the diagnostic assessments, including physical examinations, as well as CT and MRI or functional imagings, can be used by clinicians to accurately define GTVs. Based on clinical experience, a certain margin is added to GTV to account for the undetectable microscopic extensions of the tumour. This encompassing volume is labeled clinical target

volume (CTV). An additional margin is also added to CTV in order to account for the internal organ motions and daily patient set-up error. This volume, which includes both GTV and CTV, is called planning target volume (PTV) and represents the target that should optimally be covered by the prescribed absorbed dose in the final version of the treatment plan. The addition of these margins around the GTV yields 3DCRT less liable to geographic miss.

The normal structures that are identified on CT slices are usually more radiosensitive than the tumour and are called organs at risk (OAR). Depending on the scale of their vital functionality and radiosensitivity, one to several OARs are often identified for each patient and the extent of their conformal avoidance is balanced against the conformal coverage of the tumour. After defining dose-volume constraints for PTVs and OARs (which can be the same as in 2DRT), forward treatment planning is performed. This involves manual selection and alterations of the number and configurations of the beams, beam weights, and wedges until a relatively homogenous dose distribution in the target is achieved. The selection of the beam orientation is the key issue and is dictated by localization of critical OARs. In 3DCRT, each major beam encompasses the entire PTV and the aperture of each beam is adapted to the projected shape of PTV by using multileaf collimators (MLC). Simple modifications of the intensity profile of each beam can be accomplished by using dynamic or static wedges and compensation filters. As in 2DRT, photon beams with or without electron beams are often used. Figure 5. demonstrates dose distributions and beam configurations in a treatment plan prepared for 3DCRT of a NPC patient at Jubileumskliniken (JK), Sahlgrenska University Hospital.

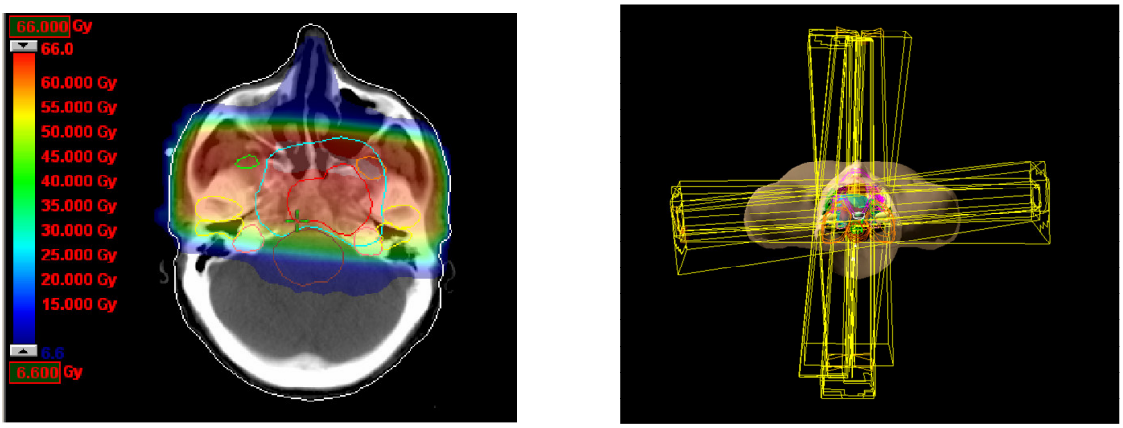

Figure 5. Beam configuration (right) and dose distributions (left) in target volumes and OARs visualized in a treatment plan prepared for 3DCRT of a T4N2M0 NPC patient. Red and turquoise coloured lines define GTV and PTV of the primary tumour. Brainstem, ears, pterygoid muscles, and TM joints are also delineated.

The major benefit of 3DCRT over 2DRT is that 3D treatment planning provides quantitative parameters for evaluation of dose distributions in target volumes and OARs. The quantitative parameters can be extracted from the available background data or dose-volume histograms (DVH), which are 1D graph presentations of the 3D dose distributions in each target or OAR. However, DVHs cannot represent spatial information, and thus visual inspection of the plans is still mandatory. The acquired parameters can be used to evaluate and optimize a single treatment plan or to compare various treatment plans prepared for the same patient. Treatment plans can thus be individualized to accommodate variations in the patient´s antomy and tumour extension. Furthermore, the extracted dose-volume data for target volumes and OARs in a cohort of patients with the same type of tumour can be correlated with treatment outcomes in terms of tumour control and RT-related side effects. Results of such correlative studies provide valuable baseline information for TCP and NTCP analysis of a particular tumour type or OAR.

It must be emphasized that in complex cases 3DCRT can run into the same limitations as 2DRT. In locoregionally advanced NPC, delivery of radical dose to the whole PTV of primary tumour is often hampered in both techniques by the radiosensitivity of surrounding critical OARs. These structures must be shielded in the boost phase of the treatment by shrinking the size of the beams or by selecting other beam orientations and qualities. Consequently, there are risks for underdosing a significant volume of the target or overdosing other OARs. Theoretically, it should be possible to come up with highly optimized treatment plans in 3DCRT for NPC patients with respect to tumour coverage and simultaneous sparing of several OARs. However, the preparation of such plans is very labor-intensive and time-consuming and involves the application of an unacceptable number of beams, making the whole process inefficient for clinical practice.

No randomized trials have compared 2DRT and 3DCRT in NPC patients. Leibel et al. (33) were the first to demonstrate that the use of 3DCRT plans in the boost phase or in tumour recurrence treatment could actually increase the mean dose to the target by 13% for the same prescribed dose compared with whole course 2DRT plans, while simultaneously decreasing the dose to the parotid glands and mandible. However, 3DCRT boost treatment of 68 nondisseminated NPC patients to a mean total dose of 70 Gy, did not improve the 5-year local control or OS rates (77% and 58%, respectively) compared with historical results using 2DRT (34). Nevertheless, reports of whole course 3DCRT of stages II-IV NPC patients who received

doses of 60-70 Gy have been promising with respect to 3 to 4-year locoregional tumour control (77%) and OS (71-90%) rates (35, 36), although the application of concurrent chemotherapy +/- accelerated irradiation in these studies might have had improving impacts.

Intensity-modulated radiotherapy

Intensity-modulated radiotherapy (IMRT) is a further development of 3DCRT. With this technique, radiation intensity in each subunit of a beam is 2D modulated so that each part of the tumour receives a unique intensity, thus making it possible to adjust the dose in OARs located in the trajectory of the beam. The sum of the non-uniform intensities from several beam orientations can then deliver more conformal dose distributions in the target and achieve better conformal avoidance of OARs. The latter increases the possibility of dose escalation within the target. Such procedures redistribute the dose within the patient so that a larger volume receives a lower dose in order to maintain a lower dose to some OARs while at the same time delivering a high dose to the target. This is called dose sharing.

The orientation of the beams in IMRT may not be as critical as in 3DCRT since the dose intensity in the regions of the beams where OARs surround the target can be lowered. Since the whole target does not need to be irradiated by each beam, the number of feasible beam orientations increases which is required in many IMRT plans in order to achieve the desired dose distribution. Another concept associated with IMRT is inverse treatment planning, in which a set of dose-volume constraints (objectives) and penalty factors for target volumes and OARs are decided on at the outset. Based on these data, a computerized optimization program calculates fluence profiles for all the beams simultaneously in order to meet the dose-volume criteria and deliver an optimized plan. Typically, dose constraints can be given for the whole volume of a target or OAR as minimum and maximum doses. By using DVHs, minimum and maximum doses can also be defined for partial volumes of targets and/or OARs. The optimization algorithm that is used for many IMRT plans is based on a least-squares objective function and an iterative Newton gradient technique.

While a major part of the planning work is automated in IMRT, clinicians and dose planners still have to decide on the appropriate dose-volume constraints. Sometimes the dose planner must “trick” the optimization system in order to get or avoid some dose in a particular region of the plan, especially when the system comes up with unexpected or unacceptable solutions. Such situations require iterative adjustment of the prescribed parameters using trial and error,

which can be time-consuming. After an optimized plan has been obtained, the intensity profile for each beam is translated into a set of leaf positions (step-and-shoot technique) or into a set of dynamic leaf motions (sliding-window technique) for an MLC incorporated in a linear accelerator. It must be remembered that, as with 3DCRT, the principles of IMRT planning, are not limited to photon therapy, but can be applied to particle treatments with electron, proton, or light ion beams (37, 38).

In general, IMRT planning is suitable for targets of complex shape located in the vicinity of vital and radiosensitive OARs, as is the case with NPC. While IMRT can be delivered as a boost treatment after 3DCRT or can be used as the sole technique in multiple phases, it has become more routine to deliver whole course IMRT with the simultaneous integrated boost (SIB) technique (39). In this technique, different targets receive different doses per fraction in the same total treatment time. By increasing the dose per fraction to higher than 2 Gy for regions expected to harbour more clonogenic cells (such as GTV), or for areas with radioresistant cells (hypoxic regions), the total delivered dose can be increased in a moderately shorter overall treatment time (OTT). Radiobiologically, the SIB technique is close to the concomitant boost technique, a form of accelerated RT that counteracts the accelerated repopulation of tumour clonogens by shortening the OTT, with beneficial effects on tumour control (40). In H & N region, it has been demonstrated that the SIB-IMRT can provide more conformal plans and better sparing of parotids than multi-phase IMRT (41). Technically, using the SIB-IMRT is preferable since only one plan has to be prepared for the whole course of treatment, thus saving time and effort in plan preparation, verification, and quality assurance. Figure 6. shows beam configurations and dose distributions in a SIB-IMRT plan prepared for a NPC patient at JK.

There are some concerns about the radiobiological effects of the SIB technique on the normal tissues embedded within the target volume, when they receive fractional doses higher than 2 Gy (42). This issue is especially critical for locally advanced NPC with tumour extension into the temporal lobes, which show clear sensitivity to high fractional doses (43).

Since mid-1990s, IMRT has been used clinically in primary treatment of NPC (2, 3, 44-46). Tables 2 and 3. summarize the published results from some of the nonrandomized retrospective studies of using IMRT +/- SIB technique in NPC patients. The results of these studies have been very encouraging, showing that when doses above 70 Gy are delivered by

the IMRT technique, improved outcomes in terms of 2 to 4-year locoregional tumour control (88-98%) and OS (83-92%) rates are possible. However, these studies reveal some impotant issues concerning IMRT of NPC patients. First, the benefit of IMRT in dose escalation to as high as 80 Gy with SIB technique might be offset by the incidence of unexpected side effects due to the radiobiological sensitivity of the normal tissues embedded within the tumour to fractionation dose. This is demonstrated by incidence of grade IV carotid pseudoaneurysm reported in one of the studies (46). Second, despite the local dose escalation, in field failure still occurs in T3 and T4 tumours. Third, despite the promising results of IMRT in parotid sparing and the reduction of the frequency of long-term severe xerostomia, RT-related side effects in other OARs are still adverse and common in NPC patients. Finally, despite the addition of CHT in these series (although not for all patients), distant metastasis remains the major site of failure. The latter observation is also confirmed in a recently published Danish report on IMRT for 20 stage II-IVb NPC patients (47). These had one-year locoregional and distant tumour control, and OS rates of 79%, 72%, and 80%, respectively.

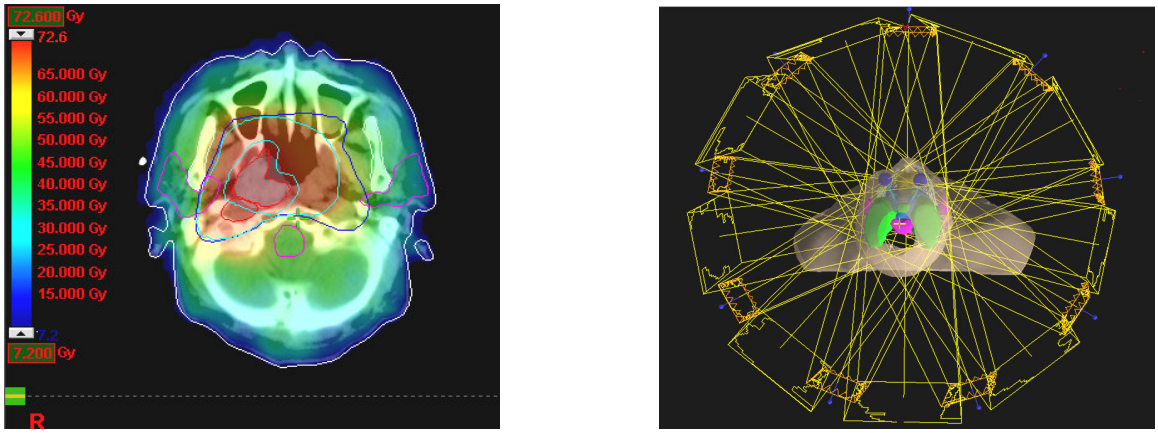

Figure 6. Beam configurations (right) and dose distributions (left) in a SIB-IMRT plan prepared for a NPC patient with T1N0M0 disease. Red contour defines GTV of primary tumour, Three PTVs are delineated with turquoise and dark blue colours, receiving 2.2, 2.0, and 1.6 Gy per fraction to total doses of 72.6, 66, and 52.8 Gy, respectively. Parotids and brainstem are also delineated.

Table 2. Survival outcomes for five clinical studies of IMRT in NPC patients.

	Lee et al. (44)	Kwong et al. (46)	Wolden et al. (45)	Kam et al. (3)	Lee et al. (2)
Year of report	2006	2006	2006	2004	2002
Population size	20	50	74	63	67
Median/mean age (years)	52	48	48	48	49
Median follow-up (months)	27	25	35	29	31
T stages	T1-T4	T3-T4	T1-T4	T1-T4	T1-T4
Dose (Gy) to GTV-T	72	76	70.2	66	65-70
Average mean dose	?	79.5	?	69	74.5
Dose/fraction (Gy)	2.4	2.17	2.34	2	2.12-2.25
Additional boost	No	No	No	12 Gy for T1-T2a 8 Gy for T2b-T4	IBT and SRS
Chemotherapy	yes	yes	yes	yes	yes
Survival rates					
Local relapse-free	----------	----------	91% (3 ys)**	92% (3 ys)†	97% (4 ys)‡
Regional relapse-free	----------	----------	93% (3 ys)	98% (3 ys)	----------
Locoregional relapse-free	88% (2 ys)•	96% (2 ys)*	----------	----------	98% (4 ys)
Distant relapse-free	90% (2 ys)	94% (2 ys)	78% (3 ys)	79% (3 ys)	66% (4 ys)
Disease-free	----------	93% (2 ys)	----------	----------	----------
Overall	----------	92% (2 ys)	83% (3 ys)	90% (3 ys)	88% (4 ys)

•One locoregional failure in T4 tumour. *All local failures in T4 tumours without chemotherapy. **All failures in T3-T4 tumours. †All failures in T3-T4 tumours without additional boost. ‡failure in one T4 tumour without chemotherapy. Chemotherapy was not administered to all patients. IBT = intracavitary brachytherapy, SRS = stereotatical radiosurgey.

Table 3. Dose to organs at risk and toxicity profile for four clinical studies of IMRT in NPC patients.

	Lee et al.* (44)	Kwong et al. (46)	Kam et al. (3)		Lee et al.* (2)	
Organs at risk						
Spinal cord (Dmax)	29 (18-37)	47 (42-50.5)	41.1 (36.4-46.7)		36.5 (9.8-46.3)	
Brainstem (Dmax)	53 (44-57)	58.3 (52.7-65.5)	50.1 (46.3-58.0)		46.3 (26.6-67)	
Optic chiasm (Dmax)	33 (12-60)	38.3 (10.9-60.7)	40.2 (9.4-60.3)		28.7 (3.6-55.7)	
Optic nerves (Dmax)	51 (39-61)	50.9 (22.9-70.6)			23.6 (7.5-67.7)	
Temporal lobes (Dmax)	----------	68.3 (59.2-76.9)	69 (64.1-71.5)			
Parotid glands (D50)	33 (28-37)		39 (29.3-65.1) (mean dose)		34.4 (7.9-72.3)	
Ears (D50)					49.1 (12.8-74.4)	
T-M joints (D50)					49.3 (19.4-79)	
Toxicity profile						
Skin						
Grade II	7	--	22		--	
Grade III	0	23	4		--	
Mucositis						
Grade II	5	--	31		47	
Grade III	13	39	25		15	
Grade IV	--	--	--		1	
Xerostomia	acute		Acute	Late	Acute	Late
Grade II	9	--	47 (g. II-III)	14 (g. II-III)	39	1
Grade III	11	--	--	--	0	0
Hearing impairment	1	21 (g. II-III)	9 (g. II-III)		5 (g. IV)	
Otitis media	6	--	--		--	
Temporal lobe necrosis	0	2 (g. I)	1 (g. I)		2 Trismus (g. I)	
Other toxicities	--	2 Carotid pseudoaneurysm (g. IV)	14 Hypopituitarism 3 Hypothyroidism 1 Osteoradionecrosis		1 Chondronecrosis (g. III)	

Toxicity grading according to CTC-V2.0 and V3.0, and RTOG & EORTC toxicity criteria. * In these series, presented doses are for 5% (D5) and 50% (D50) of organ volumes with serial and parallel structures, respectively. NPC = nasopharyngeal carcinoma, T-M = temporomandibular, g = grade of toxicity.

Radiotherapy with proton beams

The idea of using proton beams for medical treatments goes back to 1946 (48), and it was in 1954 that the first patient was treated with proton therapy at the Lawrence Berkeley Laboratory in California, USA.

The physical characteristics of proton beams differ from those of photon beams. When proton beams pass through tissue, they lose energy in atomic or nuclear interactions and slow down. Because of the energy loss, their interaction with atomic electrons increases. Dose deposition in the tissue takes place gradually until the end of the proton range, where the maximum interaction and energy transfer occurs, resulting in a rapid increase in dose deposition known as the Bragg peak (49). After this point, the dose falls off rapidly (figure 7). The depth at which the Bragg peak develops in tissue is determined by the proton´s energy. The rapid increase in the dose at a certain range and the sharp fall-off thereafter means that proton beams have great potential for RT of tumours while sparing neighbouring healthy tissues. However, while high-energy photon beams are easily produced by linear accelerators, production of high-energy proton beams requires more complicated facilities. Most proton facilities use cyclotrons that produce continuous proton pencil beams with fixed energy. However, these mono-energetic proton pencil beams are not wide enough to cover the treatment volumes and must be spread whereafter spread-out Bragg peaks (SOBP) are produced (figure 7).

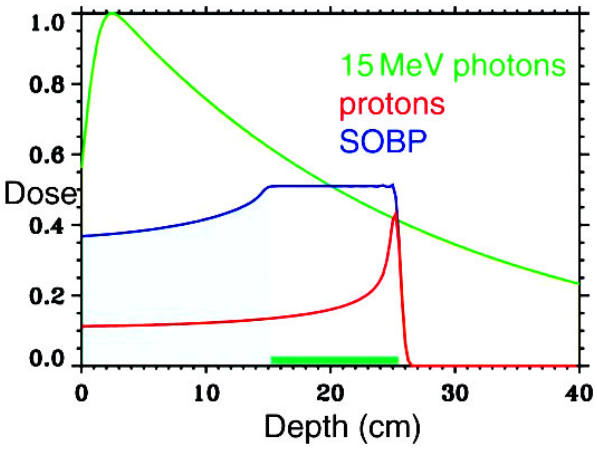

Figure 7. Central-axis depth dose curves for one mono-energetic proton beam (red line), one spread out Bragg peak (blue line) based on the mono-energetic proton beam, and 15 MeV photon beam (green line) (50).

The beams must also be shaped to the patient and target geometries. These modifications can be performed using passive or active methods (51). In the passive method (figure 8), the Bragg peaks are spread by using high atomic number scattering foils or magnetic wobbling systems. Ridge filters, range shifters, and compensators are used to obtain the desired dose distribution at a specific depth. Collimators adapt the lateral extension of each treatment beam to the shape of the beam´s eye-view of the target.

Passive-beam shaping has some disadvantages. Firstly, the depth of the dose can be tailored only to the distal end of the target, leaving a significant amount of the dose in the normal tissue in the proximity of the target volume. Second, the interaction of the proton beams with the considerable amount of material used to modulate the beams before they enter the body produces nuclear fragments, including neutrons, which produce unwanted biological effects in the entrance region.

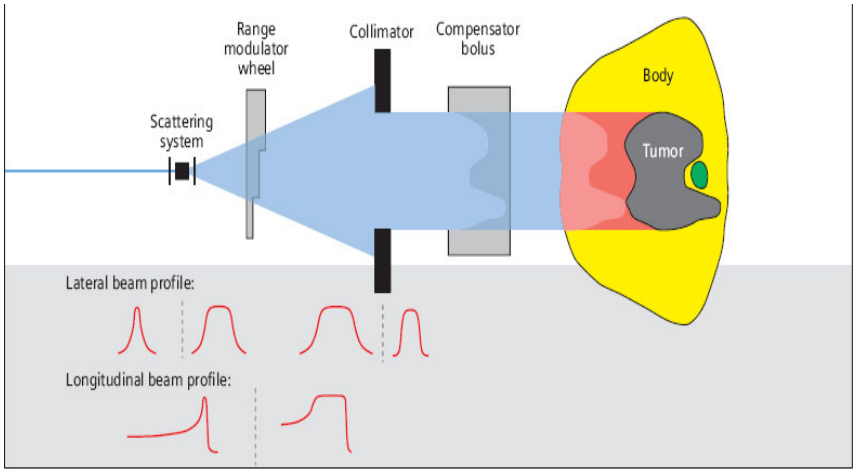

Figure 8. Principle of passive shaping of proton beams (52).

In active-beam shaping, the proton pencil beam is deflected by magnetic dipoles so that the target volume can be scanned layer-by-layer in three dimensions, the so-called active scanning (figure 9). Either static (spot scanning) or continuous (raster scanning) scanning of proton pencil beams is used to deposit the dose in the target. The optimal 3D dose distributions at the desired depth can then be achieved by using an upstream range shifter of a fixed mono-energetic proton beam produced by a cyclotron or pulsed beams of varying proton energy produced by a synchrotron. In both cases, the dose distribution can be adapted to any tumour geometry, eliminating the various materials required for beam modulation and shaping in the passive technique. However, the

equipments required for active shaping of proton beams are more complex and costly than that for passive shaping.

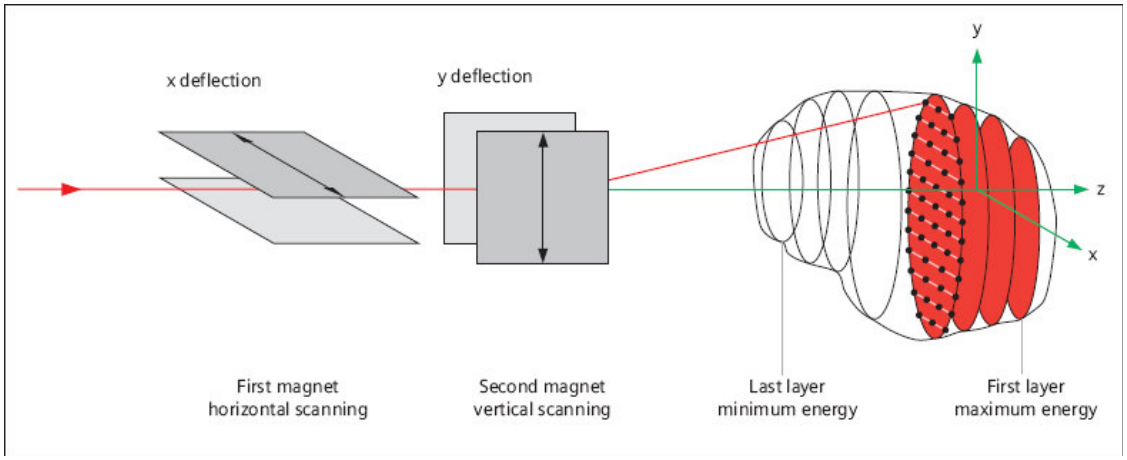

Figure 9. Principle of active beam shaping of proton beams (52).

The principles of the automated inverse treatment planning can also be applied in active proton beam scanning to optimize the proton plans and treatment (53). This approach is known as intensity-modulated proton therapy or IMPT. Clinical experience with IMPT is very limited and internationally only one proton centre, Paul Scherrer Institute (PSI) in Switzerland, uses the method.

There are some radiobiological considerations to be made in treatment planning with protons. For one thing, proton beams are biologically more effective than photon beams. The difference is defined in terms of relative biological effectiveness (RBE), which is the ratio of the dose of a photon beam (^{60}Co used as reference) to the dose of a proton beam with the same biological effect in the tissue. In proton therapy, the dose is usually prescribed in terms of the cobalt Gray equivalent (Gy_E), which is the physical dose multiplied by the RBE value. Currently, most proton therapy centres use an average RBE of 1.1 for proton beams (54-56). However, the value of the RBE is not constant, varying with the dose per fraction, the tissue irradiated , the biological endpoint, and the linear energy transfer (LET) (56). The latter quantifies the density of the ionization events in the path of a proton beam and its value increases as the energy of proton beams falls with increasing depth in the SOBP. Thus, we should expect higher RBE values at the end of the proton range (57), the end of the SOBP, with a subsequent shift of the increasing biologically equivalent dose of proton beams a few millimetres deeper into the tissue. This

phenomenon demands cautious treatment planning with proton beams when radiosensitive OARs are located in the close vicinity of target volumes receiving high absorbed doses. In these situations, the beam directions are usually chosen in such a way as to avoid the distal edge of the SOBP abutting critical OARs. For OARs that are located further away from the distal edge of SOBP, the effect of rising RBE is balanced by the steep dose fall-off of the proton beams.

Comparative treatment planning studies of proton therapy in form of IMPT versus IMRT in H & N cancers have revealed advantages of IMPT mainly in reduction of integral dose to non-target tissues and the potential for dose escalation in tumours (58-61). Figure 10. demonstrates the difference in dose distributions between IMRT and IMPT plans prepared at PSI for a case with cancer of paranasal sinus (62).

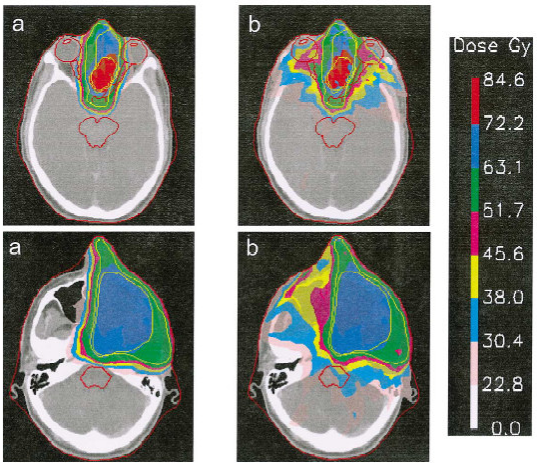

Figure 10. Dose distributions for IMRT (right) and IMPT (left) plans in two axial levels in a patient with cancer of paranasal sinus (62).

Although NPC patients are potentially suitable candidates for IMPT, there has been no report on using the technique for these patients. Nevertheless, the potential benefits of proton therapy in NPC patients have been of interest since 1980s. In a comparative treatment planning study of two nondisseminated T1 and T4 NPC patients, Brown et al. (63) demonstrated that using proton beams (passive shaping) alone or using them for the major part of the treatment in combination with photon beams, can result in more homogeneous dose distributions in the primary tumours and substantial dose reductions in adjacent tissues compared with photon therapy only. By using proton beams, the median tumour dose could also be escalated from 70 Gy to 75 Gy. Similar conclusions were reached by Noel et al. (64) in another treatment planning study that compared combined 3DCRT and proton therapy with 3DCRT only for five NPC patients with T4N0M0

tumours. Clinically, proton therapy has been used only for boost treatment of primary lesions or local recurrence in NPC patients (63-65).

Intracavitary brachytherapy

In contrast to external irradiation with photon or proton beams, with intracavitary brachytherapy (IBT) a radioactive source is positioned in the nasopharyngeal cavity. In this technique, the radiation dose falls off rapidly from the radioactive source, delivering an intended dose to the tumour but a much smaller dose to the surrounding tissue. Since position of the radioactive source is dictated by the anatomy of the nasopharyngeal cavity and because of the rapid dose fall-off from the source, IBT is not suitable for tumours of large volumes extending far beyond the nasopharyngeal cavity.

There are different methods for positioning the radioactive source in the nasopharynx. Under local or general anaesthesia, the source can be permanently implanted in the form of radioactive gold grains, ^{198}Au, or it can be placed in a custom-made mould before insertion into the nasopharynx. With these techniques, radiation is delivered with a continuous low dose rate (LDR). The disadvantages of these techniques are the necessary surgical intervention, the inconvenience for the patient of having a mould in place for several days, and the inferior radiation safety for the personnel.

Since the introduction of standardized applicators, it has become more common to use an afterloading techniqe in which a radioactive source is automatically positioned in the applicator after the latter has been put in place in the nasopharynx. With this technique, a higher dose is delivered during a very short time, leading to it being known as the high dose rate (HDR) technique. Delivery of the total dose can be divided into several sessions. Besides offering better radiation protection for the personnel, this technique is more convenient for the patients since the applicator can be removed between the irradiation sessions.

The role of IBT is only adjunctive to external RT for NPC patients and it is mainly used for dose escalation in primary treatment of early stages of the disease. This can be done as upfront treatment with a time break of 2-3 weeks after external irradiation in patients with complete response or residual tumour. When HDR-IBT with doses of 18-24 Gy was added to mean external RT dose of 61.2 Gy (2.5 Gy/fr) in T1-T2 NPC patients, Teo et al. found significant improvement in 5-year local tumour control rates from 90% to 95% compared with patients who received

external RT only (20). However, the incidence of ulceration or necrosis in the nasopharynx for the patients who received the combined treatment was also higher. In patients with persistent tumour after external RT, complementary IBT can be an option for all T stages depending on the volume of the residual tumour. In locally recurrent tumours, IBT has been used as the sole treatment or in combination with external RT (27).

Side effects of radiotherapy

Survivors of NPC have impaired health-related quality of life (66). In addition to the acute side effects of RT such as mucositis, many patients can suffer from permanent and long-term complications due to the radiosensitivity of organs adjacent to the nasopharynx and neck nodes. Moreover, combination of CHT with RT contributes further to the side effects which include ototoxicity associated with ciplatin (67). The most frequently observed late complications after RT is xerostomia reported in 90-100% of NPC patients treated with non-IMRT techniques (1, 9, 10, 68). Other common side effects include endocrinological dysfunctions, sensorineural and conductive hearing impairment, chronic otitis of middle and external ears, tinnitus, trismus, cervical soft tissue fibrosis, dysphagia, temporal lobe necrosis, cranial nerve palsies, and carotid artery stenosis (1, 9, 10, 12, 68).

Follow-up

Follow-up for NPC patients includes routine periodic examination of the original tumour site and neck, chest x-rays, MRI or CT scans, and blood work. Documentation of complete remission in the nasopharynx and cervical lymphatics is important. It is often difficult to draw the line between a slowly regressing tumour and a persistent tumour in the nasopharynx, but in most cases salvage therapy should not be delayed more than 10 weeks after completion of primary treatment (12). After documentation of complete remission, regular monitoring of the patients every 4 to 6 months for up to 5 years is recommended (12, 69). These controls are focused on detection of locoregional or distant relapse of the tumour and on RT-related side effects.

Comparative treatment planning studies in 3D radiotherapy; why they are needed, and what parameters to consider?

The introduction of intensity-modulated irradiation with photon, proton, or other particle beam therapies has been a major evolution in RT. Despite the global demand for implementation of new irradiation techniques such as IMRT and IMPT, clinical experience of using them is very narrow and their actual benefit for many tumour sites remains to be explored. The treatment planning phase in RT provides an opportunity to partially investigate the clinical potentials of these techniques without actually treating any patients.

Treatment planning studies provide information about the feasibility of certain RT techniques when certain doses are prescribed for certain tumour sites. Evaluation of the dosimetric parameters extracted from plans prepared for different RT techniques and incorporation of these data into dose-response models of TCP and NTCP can give a radiobiological platform for ranking different plans and techniques for any tumour site. It must be emphasized that the dosimetric or biological superiority of any RT technique in a treatment planning study does not necessarily mean that it will ultimately be feasible given the technical obstacles that may present during the actual delivery, quality assurance, and verification of the treatment. Nor do these results necessarily translate into any actual benefit for patients in terms of improved quality of life or survival. Nevertheless, a treatment planning study can be of value when it comes to estimating the number of patients eligible for a new RT technique and its expected costs. Comparative treatment planning studies also provide an opportunity to optimize older RT techniques by comparing them with new ones showing that good RT plans can still be prepared and delivered even when new RT techniques are not available.

The first step in comparing RT plans is visual inspection. However, in order to quantify the quality of each plan, certain physical or biological parameters must be used. For target volumes, the most useful dose parameters are the mean (Dmean), minimum (Dmin) and maximum (Dmax) doses. The average dose in the target volume is defined by Dmean, which optimally is the same as the prescribed dose. Dose distributions within the target volumes are usually not homogeneous. Dmin and Dmax are used to identify the dose in subvolumes of the target that receive much lower or higher doses than the prescribed dose (the so-called cold or hot spots). Although Dmin and Dmax can be defined as the absolute (single voxel) minimum and maximum doses in the target, it is more common to define a clinically relevant volume for these parameters. In most studies, Dmin is

defined as the dose that is received by 95% or 99% of the target volume, and is thus sometimes called D95 or D99. Similarly, Dmax is defined as the dose that is received by 5% or 1% of the target volume, and can thus be presented as D5 or D1. The ratio of the difference between Dmax and Dmin to Dmin (or Dmean) is called the inhomogeneity coefficient (IC) and reflects the homogeneity of dose distribution within a target. Ideally, the desired ratio should be zero, indicating that the whole target is covered by the prescribed dose with no cold or hot spots. In practice, the IC values should be kept as low as possible. Treatment plans can also be evaluated based on volume parameters such as V95 and V105, presenting the relative volumes of the target that are covered by ≥95% and ≥105% of the prescribed dose. In a perfect plan, these values should be 100% and 0%. The conformity index (CI) is used to evaluate the conformity of a plan. In the basic concept, CI is the ratio of the absolute volume of the prescribed isodose in the whole body to the volume of the PTV. Ideally, the value of CI should be unity. In many cases, the prescribed isodose does not cover the target totally, and the value of the above equation can be misleading. To circumvent this problem, one can use the absolute volume of the PTV that is covered by the prescribed isodose instead of the PTV in the equation.

The degree of conformal avoidance in treatment plans for OARs can be measured by calculating Dmean and Dmax for the organs. Commonly, Dmean is used for OARs with mainly parallel structures (70), and Dmax is used for OARs with mainly serial structures (71).

The significance of the physical parameters derived for target volumes and OARs in any plan is clearer if they can be translated into certain radiobiological effects such as TCP and NTCP. Currently, these endpoints can be estimated using radiobiological models that incorporate the available clinical data regarding the dose-volume characteristics of different tissues. Although these are only statistical models that fit observed clinical data and their predictive reliability is yet to be proven, they can be used to complement clinical experience in radiobiological ranking of treatment plans.

The poisson model is most frequently used in calculating TCP (72). Generally, TCP models assume that local control is achieved if all clonogenic cells are destroyed by radiation (71). With Poisson statistics, the probability of that there are no surviving clonogens can be predicted by knowing the initial number of clonogenic cells and the surviving fractions (SF) of these cells after receiving a certain uniform dose. The surviving fraction for any tumour can be calculated from linear-quadratic models if it´s radiobiological parameters of α and β, and α/β, are known. These

parameters can replace SF in TCP calculations. In a population with variable radiosensitivity, a mean α value and its standard deviation (σ) are also needed. In order to calculate the TCP with poisson statistics for non-uniform dose distribution in a tumour (as in clinical practice), the tumour is approximated by many subvolumes that are small enough to receive a uniform dose but large enough for the poisson statistics to be valid. This can be done by using differential DVHs that can be extracted from treatment plans. Since the biological effect of variations in dose per fraction within the tumour with high values of α/β is small, the β-term can be neglected in calculations. In summary, by knowing the values of the mean α, σ, α/β, and the initial clonogenic cell density and by using differential DVHs, the TCP for the target volumes can be calculated and compared for different plans. If required, the effect of accelerated tumour repopulation can also be incorporated into these TCP calculations.

Due to the conceptual uncertainties in TCP modeling and their computational demands, a new concept, the Equivalent uniform dose (EUD) has been introduced (73). The EUD is defined as the dose that, when distributed uniformly across the target volume, can lead to the same biological effect as the given non-uniform dose distribution. It has been shown that the EUD value is bounded above by the Dmean and below by the Dmin. In highly homogeneous plans, the EUD value is closer to the Dmean and in more heterogeneous plans, it is closer to the Dmin. The basic parameters that are required for calculating the EUD for a specific tumour are volume fractions at various dose levels (derived from DVHs) and SF at 2 Gy (SF2). In a way, the EUD is an intermediate quantity between purely biological endpoints and physical parameters. The concept of EUD is not limited to tumours and it can also be applied to normal tissues, in the so-called generalized EUD (70).

Among radiobiological models for NTCP calculations, the Lyman-Kutcher-Burman (LKB) model is commonly used (74-76). This model describes the sigmoidal dose-response curve of normal tissues and predicts the probability of complications in a partially uniformly irradiated organ. Since in most situations organs are irradiated nonuniformly, a reduction scheme is incorporated in this model to reduce a DVH to a reference dose delivered to an effective fractional volume (75). This can be done by using differential DVHs. The LKB model has three parameters: D_{50}, m, and n. D_{50} represents the dose at which there is a 50% chance of complication when the whole organ is uniformly irradiated; m controls the slope of the dose-response curve at D_{50}, the steepest part of the curve; and n determines the dose-volume dependence of a tissue and thus accounts for

differences in tissue architecture (higher values correspond to a more parallel architecture). These three parameters are tabulated for different organs and specific endpoints, originally based on the clinical tolerance data published by Emami et al. (77). However for some organs, recent studies of 3D dose distribution and best-fit analysis of clinical data have given different values for these parameters (78, 79).

MATERIALS AND METHODS

The description of materials and methods for papers I and IV is done separately from papers II and III due to major differences in their constructions.

Paper I and IV:

Study population

From 1991-2002, a total number of 81 patients diagnosed with NPC were registered at the JK, Sahlgrenska University Hospital and the Oncology Centre (OC) for the Västra Götaland health region. Twelve of these patients had tumour histologies other than SCCs. These included 4 rhabdomyosarcoma, 3 plasmocytoma, 2 malignant melanoma, and 3 others. Seven patients had been referred to JK from other regions for IBT in primary treatment of the disease or because of local relapse. Five patients from the southern part of the Västra Götaland health region were referred to the Department of Oncology in Lund for therapy. Three patients established contacts with JK only for consultation or check-ups. During this period, one patient who had been treated at JK before 1991 required re-treatment for a local relapse. No data could be found for a patient who was registered at OC only. In total, 52 patients with a diagnosis of SCC of NPC were referred to JK for primary treatment during the chosen period and were included in the first study. Of these, two patients were excluded from treatment and outcome analysis due to refusal of treatment or early interruption of treatment. One of the remaining 50 patients had M+ disease at diagnosis, but received neoadjuvant CHT and radical dose of external RT locoregionally. This patient lived 17 months after treatment and was therefore included for evaluation of therapy-related side effects. However, he was excluded from the survival analysis. We chose 1991 as the starting year for the study since from this year on, 3DCRT was introduced for all NPC patients at JK. We intended to allow for a minimum of two years for follow-up of the patients. Since data collection and registration started in 2004, the end of 2002 was set as the final date for the patients to be included. For the research reported in paper IV, an attempt was made to retrieve original biopsy materials for all SCC NPC patients registered at JK during this period. Forty-five patients had both adequate material for analysis of biomarkers (45 for LMP1 and 44 for Ki-67, cyclin-B1, and EGFR) and had received therapy with curative intent, and so these were selected. All but three of these patients were also included in the first study.

Patient workup

In the Västra Götaland health region, it is recommended that all newly diagnosed patients with H & N cancers be referred to a multidisciplinary conference held weekly at Sahlgrenska University Hospital. At these conferences, patients are evaluated by oncologists, H & N-, dental-, and plastic surgeons, radiologists, pathologists, and nutritionists in order to decide on the optimal treatment strategy. The baseline workup of the patients for tumour staging and therapy recommendations includes a complete medical history, physical examination, review of biopsy materials, fibreoptic endoscopy of the upper aerodigestive tract, CT and/or MRI of whole H & N region, chest x-rays and blood profiles. Complementary examinations such as bone scintography or chest and abdominal CT scans are only performed when clinically indicated. Recently, detection of the EBV genome in biopsy materials is also recommended.

Treatment policy

The principal modality in primary treatment of all nondessiminated NPC patients at the JK is radical external RT. Prior to the introduction of IMRT, all NPC patients were also offered IBT after termination of the external RT in order to enhance the dose to at least some part of the primary tumour. Chemotherapy is reserved for patients with locoregionally advanced tumours.

Chemotherapy

Paper I:

Chemotherapy was delivered to 36 patients, all with stages ≥ IIb. Neoadjuvant CHT, mainly with a combination of cisplatin and 5FU, was delivered in one to three courses every third week to 33 patients. The objectives for using neoadjuvant CHT were to reduce the risk of distant metastasis and to shrink the primary tumour before external RT, thereby increasing the safety margin between the bulk of the tumour and the intended target volume. The latter could theoretically improve the probability of local tumour control. Three patients were accrued in the phase I trial involving administration of Tegafur-Uracil (UFT) and leucovorin concomitant with hyperfractionated accelerated RT (HART) in advanced H & N cancer, and so they did not receive neoadjuvant CHT. Chemotherapy was avoided in nine patients with stage II-IV disease due to advanced age, compromised performance status, and pretreatment noise-induced hearing loss. The dose or type of CHT agent, or the number of planned courses, was modified in 17 patients who received

neoadjuvant CHT due to the side effects or pretreatment conditions such as advanced age, hearing impairment, and cardiac morbidity.

Paper IV:

Chemotherapy was delivered to 32 patients mainly with neoadjuvant approach (29 patients). Majority of the patients received combination of cisplatin and 5FU delivered in one to three courses every third week. Three patients received UFT/leucovorin concomitant with RT.

Radiotherapy

Before treatment planning for external RT, the craniocervical part of each patient was immobilized with perspex shells or thermoplastic masks and headrests. Then, planning CT scans of the H & N region were acquired in treatment position. After delineation of the GTV of the primary tumour (GTV-T) and lymph node metastases (GTV-N), a margin of 1.5-2 cm with some modifications was added to these GTVs to construct PTV-Ts. PTV-N was delineated for the adjuvant volume of cervical lymph node stations and included bilateral lymph node levels of II to V, including medial parts of supraclavicular fossae.

External RT was planned and delivered in 2 to 3 phases with 3DCRT technique. For the first phase, two lateral opposed photon beams were used for the nasopharynx and upper neck. In cases where the nasal cavity was also involved, one or two heavy fluenced anterior beams were also added. At the level of the upper larynx, the above fields were matched to one anterior or two AP-PA photon beams covering the lower neck. In most cases, the spinal cord and larynx were shielded. The subsequent phases were off-cord treatments and were planned individually for each patient using photon and electron beams covering PTV-Ts. The doses for PTVs were prescribed at the reference point recommended by ICRU-50/62 (32), aiming for dose homogeneity within -5% and +7% of the prescribed dose.

Paper I:

For 32 patients, external irradiation was delivered as a split course HART, 1.7 Gy/fr twice a day (with minimum of 6-hour interval), five days a week. PTV-T of the primary tumour and lymph node metastases received a median dose of 61.2 Gy (range, 35.7-64.9 Gy) and 64.6 Gy (range, 35.7-68 Gy), respectively and PTV-N received 40.8 Gy. The median OTT was 33 days (range, 30-

38 days) including a mid-course break of 5-12 days (median, 9 days) planned at 34 Gy. Two patients received a subtotal treatment of 56.1 Gy and 35.7 Gy due to previous RT of H & N region and treatment refusal, respectively.

For 18 patients, external RT was given conventionally (CRT) with 2 Gy/fr, once a day, and 5 days a week. The prescribed doses for PTV-Ts of primary tumour and lymph node metastases were 54-68 Gy (median, 66 Gy) and 58-68 Gy (median, 66 Gy), respectively. PTV-N received 50 Gy. The median OTT for these patients was 46 days (range, 37-62 days). In four patients, CRT was converted to hyperfractionated treatment of 2 Gy x 2 for the PTV-T of the primary tumour in the last phase of the treatment.

The rationale behind using HART was to reduce the time for accelerated repopulation of tumours by reducing the OTT. This approach has been shown to be beneficial for local control of H & N cancers (80-82). The splitting of the daily dose by the hyperfractionation scheme in HART, gives a lower dose per fraction to normal tissues, which are more sensitive than tumour cells to the fractionation dose. The minimum 6-hour interval between the daily fractions also allows for repair of sublethal damage in normal tissues. The time break in the split course schedule is intended for the recovery of acute reactions in mucosa (83). Since HART is associated with higher rates of acute side effects (82), the treatment is usually avoided in elderly. In the cohort of patients in paper I, the median ages in the HART and CRT groups were 54 and 70 years, respectively. In the early 1990s and early 2000s, relatively more patients were treated by CRT. The reason was the general implementation of HART for H & N cancer patients at JK between these two periods. However, reports of the increased risk of side effects with HART, and especially temporal lobe necrosis in NPC patients (10), led to CRT again being recommended for these patients.

Forty patients received IBT, with a median gap of 15 days after termination of external RT. The distribution of T stages among these patients was as follows; T1 in 13, T2a in four, T2b in seven, T3 in eight and T4 in another eight patients. Advanced age, technical difficulties, patient refusal, inadequate dose, or early death after external RT and M+ disease were among the reasons that IBT was not delivered in remaining 10 patients. Up to 1994, this treatment was delivered to eight patients using the LDR technique. Thereafter, IBT was delivered to the remaining 32 patients using HDR technique with a standard applicator. In both techniques, ^{192}Ir was used as the irradiation source. For delivery of IBT with the LDR technique, a custom-made mould or commercial applicator (Nucletron®) was used. The prescribed dose ranged between 7-12 Gy. In

the HDR technique, a Nucletron® or Gammamed® standard applicator was used. The prescribed dose was usually 6-7 Gy divided into two sessions and delivered in 1-2 days. In both techniques, the doses were prescribed at 5-13 mm from the surface of the mould or applicator, which was positioned in the nasopharynx under general anaesthesia.

For statistical evaluation of the impact of absorbed dose on treatment outcomes, the total physical dose for each patient was calculated by summation of all the delivered doses from external RT and IBT. The median total physical dose for the whole cohort (M+ patient excluded) was 69.1 Gy (range 35.7-74.6 Gy). Due to the variability of the prescribed doses, fractionation patterns and OTTs, the equivalent dose in 2-Gy fractions with α/β of 10 ($EQD2_{10}$) and $EQD2_{10}$ corrected for OTT and accelerated tumour repopulation ($EQD2cor_{10}$) were also calculated for both total doses of external RT ($EQD2_{10\text{-}XRT}$ and $EQD2cor_{10\text{-}XRT}$) and external RT+IBT ($EQD2_{10\text{-}XRT/BT}$ and $EQD2cor_{10\text{-}XRT/BT}$) where available. For external irradiation, $EQD2cor_{10\text{-}XRT}$ values were computed from the corresponding $EQD2_{10\text{-}XRT}$ values by correction for accelerated tumour repopulation with assumption of dose loss of 0.5 Gy/day after 28 days (20, 84). Computed EQD2 values from IBTs were simply added to corresponding $EQD2_{10\text{-}XRT}$ and $EQD2cor_{10\text{-}XRT}$ values when calculating $EQD2_{10\text{-}XRT/BT}$ and $EQD2cor_{10\text{-}XRT/BT}$ values. No correction was performed for accelerated tumour repopulation during the time gap between external RT and IBT assuming that tumour cells would likely fall back into a slow rate of pre-RT proliferation shortly after a complete course of external RT (20). $EQD2_{10}$ values were calculated according to three formulas written below (85).

Equivalent dose in 2Gy fractions:

$$EQD_2 = D\frac{d+\frac{\alpha}{\beta}}{2+\frac{\alpha}{\beta}}$$

Equivalent dose in 2Gy fractions for fractionated radiotherapy:

$$EQD_2 = D\frac{d\left(1+H_m\right)+\frac{\alpha}{\beta}}{2+\frac{\alpha}{\beta}}$$

Equivalent dose in 2Gy fractions for continuous low-dose-rate radiotherapy:

$$EQD_2 = D\frac{dg + \frac{\alpha}{\beta}}{2 + \frac{\alpha}{\beta}}$$

D is total physical dose for each modality, d is dose delivered per fraction, α and β quantify the fractionation sensitivity of the tumour in the linear-quadratic model of cell survival, *Hm* and g are correction factors for incomplete repair in hyperfractionation and continuous irradiations, respectively.

The median values for $EQD2_{10\text{-}XRT}$ and $EQD2cor_{10\text{-}XRT}$ were 63 Gy and 57.7 Gy, respectively. The corresponding values for $EQD2_{10\text{-}XRT/BT}$ and $EQD2cor_{10\text{-}XRT/BT}$ were 68.4 Gy and 64 Gy, respectively (The patient with M+ disease was excluded).

Paper IV:

External RT was delivered with HART in 30 patients and CRT in 15 patients with a median dose of 64.3 Gy (range 54-68 Gy). Thirty-seven patients received IBT (LDR or HDR techniques) with a median dose of 6 Gy (range 4.5-12 Gy). The median total physical dose delivered for the whole cohort was 68.2 Gy (range 54-74.6 Gy).

Patient follow-up

The median follow-up for the patients in paper I and IV were 4.1 and 5.3 years (range for both studies; 0.1-12.5 years), respectively. Patients who received neoadjuvant CHT were assessed before each course. During external RT, most of the patients were evaluated weekly. The first follow-up visit was scheduled 6-8 weeks after termination of RT and thereafter every 3-4 months for the first 2 years. In subsequent years, the visit intervals were increased to every 6-12 months. The patients were followed-up for a minimum period of five years by an experienced oncologist. Some patients had longer follow-ups due to protracted late side effects and preference of their physician at JK or referring hospital. Post-therapeutic CT scan or MRI of H & N region were scheduled usually within six months after completion of treatment and were repeated regularly if persistent tumour was suspected. Local biopsies were performed mainly in case persistent or recurrent tumour was suspected. In case of tumour progress or relapse at any site, patients were

treated at JK. Documentation and management of side effects of RT was also included in surveillance of the patients.

Data collection and evaluation

Available medical records of the patients at JK were reviewed with respect to demographic and tumour specific data, as well as information on treatment and treatment outcomes. In recent years, an electronic patient record system (Melior®) has made it possible to review the medical records from other specialist areas in our hospital to determine whether patients have sought help from them. These records were especially useful when it came to the detection and registration of RT-related side effects. For the patients referred to JK from other hospitals, copies of the medical records from those hospitals were reviewed. However, a lack of regular correspondence between JK and some of ENT or odontology clinics may have resulted in insufficient data on side effects. Regional guidelines prescribed that all confirmed cases of tumour recurrence were to be discussed with JK. Death records were obtained from the national death registry. All relevant data were updated at the time of data analysis for paper I (November 2005) and paper IV (April 2007).

Tumour staging

Between 1991 and 2002, NPC cases were classified and staged according to the UICC/AJCC 1992 system. In some cases a nodal classification system from other H & N sites was used. After review of the medical records, including radiology reports, all NPC patients enrolled in the four studies were reclassified and restaged according to the UICC/AJCC 1997 system. Figure 11. demonstrates the distribution of different tumour stages before and after restaging.

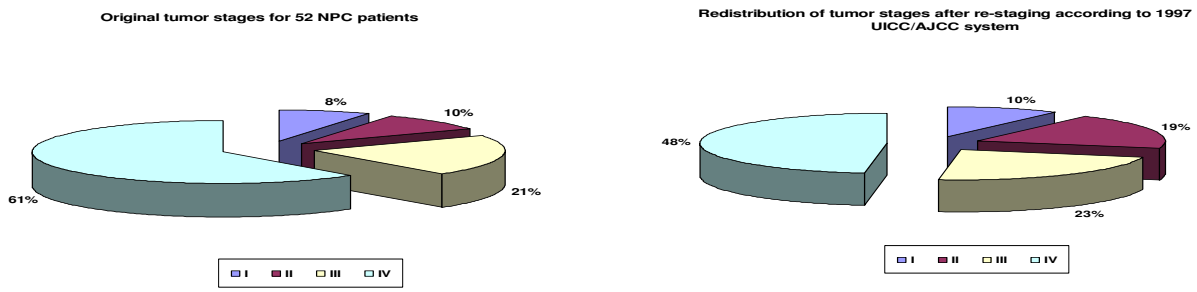

Figure 11. Distribution of tumour stages for 52 NPC patients before and after restaging according to UICC/AJCC 1997 system

Histology

Histologically, tumours were also reclassified in terms of the three WHO types (11). In paper I, this reclassification was based on pathology reports. Well- and moderately well-differentiated SCCs were regarded as WHO type I, and poorly differentiated SCCs (including transitional cell carcinomas) and undifferentiated carcinomas (including spindle cell carcinomas) were categorized as WHO type II and III, respectively. For statistical analysis, tumours were divided into two groups, WHO type I and WHO types II-III. In paper IV, all tumour biopsies were re-evaluated by an experienced pathologist (B.M.) partly for a precise histopathological classification of these according to WHO, and partly for verification of the quality of the samples for immunohistochemical (IHC) analysis. In this study, only two patients had a WHO type I tumour. Hence, for statistical analysis, we decided to divide the patients into two groups of WHO type I-II and WHO type III tumours.

Treatment-related toxicity

The treatment-related toxicities reported in paper I, were based on the available data in medical records of the whole cohort, and telephone interviews with the living patients. Maximum grade of toxicity was documented for each patient and site. Grade of xerostomia was also recorded from the last follow-up visits or telephone interviews with patients. All acute and late toxicities were graded according to Common Terminology Criteria For Adverse Events, version 3.0 (CTCAE v3.0) (86) except for xerostomia, trismus and tinnitus, which were graded according to LENT-SOMA grading scale (87). Tables 4 and 5 show the grading scales for majority of the side effects according to the two systems. Because of the missing data for some patients or sites, the results reported in paper I should be considered as minimum crude toxicity rates.

Table 4. Common Terminology Criteria for Adverse Events v3.0 (CTCAE v3.0) (86).

Toxicity	**Grade I**	**Grade II**	**Grade III**	**Grade IV**	**Grade V**
Acute mucositis	Erythema	Patchy ulcerations or pseudomembranes	Confluent ulcerations or pseudomembranes, bleeding with minor trauma	Tissue necrosis, significant spontaneous bleeding, life-threatening consequences	Death
Hearing Impairment	----------	Hearing loss not requiring hearing aid or intervention	Hearing loss requiring hearing aid or intervention	Profound bilateral hearing loss (> 90 dB)	----------
Otitis externa	Erythema or dry desquamation	Moist desquamation, edema, enhanced cerumen or discharge, tympanic membrane perforation, tympanostomy	Mastoiditis, stenosis or osteomyelitis	Bone or soft tissue necrosis	Death
Otitis media	Serous otitis	Serous otitis, medical intervention indicated	Otitis with discharge or mastoiditis	Bone or soft tissue necrosis	Death
Hypothyroidism	Asymptomatic	Symptomatic, not interfering with ADL, medical intervention indicated	Interfering with ADL, hospitalization indicated	Life-threatening myxedema coma	Death
Temporal lobe necrosis	Asymptomatic, radiographic findings only	Symptomatic, not interfering with ADL, medical intervention indicated	Symptomatic and interfering with ADL, hyperbaric oxygen indicated	Life-threatening, disabling, operative intervention indicated	Death

Table 5. Late effects of radiotherapy on normal tissues/subjective, objective, management, and analytical (LENT-SOMA) scoring scales (87).

Toxicity	**Grade I**	**Grade II**	**Grade III**	**Grade IV**
Xerostomia	Occasional dryness Norma moisture ----------	Partial but persistent dryness Scant saliva Occasional saliva substitute, sugarless gum, sialogogues	Complete dryness, non-debilitating Sticky, viscous saliva, absence of moisture Frequent saliva substitute or water, sugarless gum, sialogogues	Complete dryness, debilitating Coated mucosa, absence of moisture Needs saliva substitute or water in order to eat, sugarless gum, sialogogues
Tinnitus	Occasional	Intermittent	Persistent	Refractory
Trismus	Noted but unmeasurable	1-2 cm opening	0.5-1 cm opening	< 0.5 cm opening

Immunohistochemistry of biomarkers (paper IV):

All 45 patients had adequate biopsy material for LMP1 analysis. Forty-four specimens provided adequate material for Ki-67, cyclin-B1, and EGFR analysis.

From the formalin-fixed and paraffin-embedded tissue blocks of the specimens, 4-µm cross-sections were prepared. After deparaffinization and rehydration in order to retrieve the antigenicity, the sections were treated with TRIS/EDTA buffer (pH 9.0) for Ki-67 and LMP1, and citrate buffer (pH 6.0) for cyclin-B1 staining, and heated at boiling point for 20 minutes using a microwave oven. For EGFR staining, the sections were treated with protease XXIV (pH 7.6) at 37ºC for 20 minutes. Then, the sections were cooled and washed in phosphate-buffered saline (PBS) before immunostaining. The monoclonal mouse anti-human primary antibodies used for the four markers were as follows: clone MIB-1 (DAKO, Glostrup, Denmark), dilution 1:100, for Ki-67; clone E30 (DAKO, Glostrup, Denmark), dilution, 1:25, for EGFR; clone 7A9 (NovoCastra, Newcastle, United Kingdom), dilution 1:40, for cyclin-B1; and clone CS 1-4 (DAKO, Glostrup, Denmark), dilution, 1:100, for LMP1. All tissues were incubated with the primary antibody for 25

minutes at room temperature. Endogenous peroxidase was blocked with PBS and nitrogen peroxide, whereafter a dextran secondary antibody-peroxidase complex kit (DAKO En Vision) employing the capillary gap staining technique with the automated TechMate 500 immunostaining system was used. Diaminobenzidine was used to visualize the stained tissues. The sections were counterstained with hematoxylin. The positive controls with known positive immunoreactivity were tonsil cancer specimens for Ki-67 and cyclin-B1, basal cells of a dermal tissue for EGFR, and EBV-infected human tissue for LMP1. Stainings without primary antibodies were used as negative controls.

After IHC staining, the representative areas of the tumour tissue in each section were scanned by a pathologist (B.M.) under low-power light microscopy (x 100). They were then scanned at x 250 magnification whereafter they were photographed with a digital camera (Leica DC 100; Leica, Heerbrugg, Switzerland) for analysis on a computer screen. For most of the patients, at least two separate fields were photographed and each field corresponded to an area of one mm^2. In two patients, only one field was available for evaluation due to a limited amount of tumour tissue. All slides were scored based on the tumour population only. For more accurate analysis of the staining of the cytoplasm or nucleus, all digital images of the fields were also transferred to Microsoft Paint program and viewed with inverted colours. The analysis of the slides was performed independently by two researchers (B.M. and Z.T.K.), both blinded to the clinical features and treatment outcomes.

The Ki-67, cyclin-B1 and EGFR labeling indices (LIs) were defined as the percentage of tumour cells expressing nuclear, nuclear/cytoplasmic, and membrane immunoreactivity, respectively. Overexpression of Ki-67 was defined as a value greater than or equal to the median LI of the population. A cutoff value of $\geq$ 15% was set for cyclin-B1 overexpression, which almost corresponded to its median LI in the whole series. For EGFR immunoractivity, both the extent and the intensity of the staining were evaluated. EGFR overexpression was defined as EGFR expression with an LI $\geq$ 50%. The EGFR staining intensity was graded semi-quantitatively in four groups, of none (0), weak (1), moderate (2), and strong (3), based on the intensity of the majority of the stained cells. Due to nonhomogeneous staining in some specimens, and for more accurate quantification of the EGFR staining, the digital images were also processed using Adobe Photoshop 7.0 histograms (Adobe Systems, Inc., San Jose, CA, USA) whereafter mean luminescence intensity (MLI) scores were determined for each image and patient. The

luminescence intensity scores could vary from 0 and 255 for each pixel of an image. Lower MLI scores corresponded to more intensely stained specimens and higher scores were related to lighter shades of staining.

LPM1 positivity was considered when immunoreactivity was displayed in the membrane, cytoplasm, or, in some cases, the nuclear components of the tumour cells.

Paper II and III:

Study population

For these two comparative treatment planning studies, we chose eight NPC patients randomly from the historical material, independent of the time for their actual treatment. The only clinical criteria for selection of these patients were equal presentation of every T stage, variation of the nodal stage from N0 to N3b in the whole cohort, and that they had adequate radiological examinations in the initial workup. The original therapeutic CT scans of the patients were used for all treatment plannings. Therapeutic CT scans for RT planning at JK were 7 mm in thickness. However, after 2002, JK decided to acquire CT scans with 5 mm thickness for H & N cancer patients. Since the geometric information and thus dose calculation is more accurate when CT slices are thinner, we decided to include NPC patients with 5 mm CT slices when available. Hence, three of the patients in these two studies were registered at JK after 2002. The TNM stages for the cohort were; $T_1N_0M_0$; $T_1N_1M_0$; $T_{2a}N_{3a}M_0$; $T_{2b}N_{3b}M_0$; $T_3N_2M_0$; $T_3N_{3b}M_0$; $T_4N_1M_0$; $T_4N_2M_0$.

Definition of target volumes and OARs

All volumes in paper II and III were delineated by the same radiation oncologist (Z.T.K.). In paper II, Varian´s Eclipse™ treatment planning system was used for both delineation of volumes and preparing all treatment plans. Gross tumour volumes of primary tumour (GTV-T) and all macroscopic nodal metastases (GTV-N) were re-delineated on the original therapeutic CT slices after reviewing the available clinical data including diagnostic CT and/or MRI. Three sets of CTVs were defined for each patient. CTV-T comprised GTV-T without any margin. CTV-TN was defined as the volume encompassing both GTV-T and GTV-N (when macroscopic nodal metastases was presented), with a 10 mm margin in all directions; the whole of the nasopharynx cavity was also included in this volume. CTV-N consisted of the volume of bilateral cervical

lymph node stations in levels Ib to V, medial supraclavicular fossae, retro/parapharyngeal spaces, the posterior third of the nasal cavity and maxillary sinuses, inferior sphenoidal body, clivus, and pterygoid fossae. The central volume of the neck from the level of the vocal cords caudally could be excluded from any target volume since there was no evidence of tumour extension in this region in any of the patients. In order to account for setup errors and patient movements, three sets of PTVs (PTV-T, PTV-TN, and PTV-N) were also defined by adding a 5mm margin to each corresponding CTV. All PTVs and CTV-TN were modified wherever they encountered neural tissues or bony structures without evidence of tumour infiltration. Besides the standard OARs (spinal cord, brainstem, temporal lobes, the optic apparatus and parotid glands), the inner and middle/external ears, TM joints, pituitary and thyroid glands, larynx and mandible were all delineated for each case.

For the purposes of study III, the treatment planning system, VIRTUOS, available at the German Cancer Research Center (DKFZ), Heidelberg, Germany was used. Due to technical incompatibilities between Eclipse and VIRTUOS, only original CT data sets with no structure included could be transferred between the two systems. Hence, all the previously mentioned volumes had to be re-delineated for each patient. Principally, all target volumes were defined the same as in paper II. However, some modifications were introduced in paper III. PTV-T was omitted in this study with assumption of stereotactical delivery of both IMRT and IMPT plans and thereby reduced risk of set-up errors. The mean volumes for GTV-T, PTV-TN, and PTV-N in paper III were 24.4 cc, 287.8 cc, and 450.3 cc, respectively. The mean values for the same targets in paper II were, 23.5 cc, 322.6 cc, and 466.3 cc, respectively.

In delineation of OARs in paper III, oral cavity, skin, and cerebellum/posterior brain tissue up to the level of the clinoids were also added for evaluation of dose distributions only. As hypopharynx and upper esophagus are located in the close vicinity of larynx, these structures were delineated altogether and named larynx/esophagus.

Dose prescriptions, dose-volume constraints, and treatment plannings:

In paper II, two sets of plans were prepared for each patient. One with SIB-IMRT technique (referred as simultaneous integrated multi-target, SIMT-IMRT in the paper) and the other with highly-optimised 3DCRT combined with IBT. In the IMRT plans, the prescribed mean doses for PTV-T, PTV-TN, and PTV-N were 72.6 Gy, 66 Gy, and 52.8 Gy delivered simultaneously in 33

fractions, thus 2.2 Gy, 2.0 Gy, and 1.6 Gy per fraction, respectively. The expected OTT was 45 days with five days a week administration of RT. IMRT plannings and optimizations were performed using Eclipse™ treatment planning system and Helios™ optimization program (Varian Medical Systems). For all cases nine coplanar, equally spaced, 6 MV photon beams were used. Based on the user-defined dose/dose-volume constraints and penalty factors for the target volumes and OARs, Helios™ used an iterative gradient technique in order to improve the 3D dose distributions and minimizing the objective functions. In the optimization process, only soft constraints were used. The optimized intensity profile for each beam was used to simulate sliding window delivery technique prepared for a Varian linear accelerator with an 80-leaf MLC.

In the combined plans, 66 Gy and 46 Gy (2 Gy/fr, five days a week) were prescribed to the ICRU reference point for PTV-TN and PTV-N, respectively. PTV-T would also receive a further boost of 6 Gy (3 Gy x 2, 6-hour interval) by HDR-IBT two weeks after termination of 3D-CRT, reaching a total dose of 72 Gy. Depending on the thickness of the soft palate, IBT was planned to be delivered at 5-10 mm from the surface of an applicator, so that no more dose than the prescribed dose would reach the oral surface of this structure. The expected OTTs for PTV-T, PTV-TN, and PTV-N were 60, 45, and 31 days. Table 6. presents radiobiological equivalencies of the prescribed doses in 2 Gy fractions (EQD2) applying linear quadratic models corrected and uncorrected for accelerated tumour repopulation, showing slight dose-escalation to PTV-T in IMRT plans.

Table 6. Radiobiological equivalent doses for the prescribed physical doses in SIB-IMRT and 3DCRT+IBT (paper II).

Target volume	SIB-IMRT Dose	SIB-IMRT (EQD2/EQD2$_{cor}$)	3DCRT+IBT Dose	3DCRT+IBT (EQD2/EQD2$_{cor}$)
PTV-T	72.6	73.8/63.6	72	72.5/62.3
PTV-TN	66	66/55.8	66	66/55.8
PTV-N	52.8	51/40.8	46	46/44.2

EQD_2 / EQD_{2cor} = radiobiological equivalent dose in 2 Gy fractions uncorrected / corrected for accelerated tumour repopulation (α/β = 10, lag time= 28 days, 0.6 Gy/day dose loss. Overall treatment time 45 days for all PTVs in IMRT and 45 and 31 days for PTV-T/PTV-TN and PTV-N in 3D-CRT + IBT plans. Accelerated repopulation of clonogenic tumour cells between 3DCRT and IBT is assumed to be zero). All doses are in Gy.

For 3DCRT, two-phase highly optimized forward planning was used. The first phase was planned to 46 Gy using mainly 6 MV photon beams shaped with MLC and individual blocks in order to

obtain good dose conformity. In general, two laterally opposed beams covered the nasopharynx and upper neck. The mid to lower neck was covered with two to four AP-PA beams with central shielding from the level of the vocal cords extending caudally. Low fluenced beams with suitable shapes were also added for plan optimization. The second phase was planned to 66 Gy, applying a complex configuration of photon and electron beams. On average, 13 beams were used for each 3D-CRT plan in order to comply with the same dose-volume constraints as for IMRT plans.

The dose distributions from IBT sources were reconstructed on the same CT slices as used in 3DCRT treatment planning. Firstly, the actual IBT treatment data including source stopping positions, dwell times, and orthogonal X-ray images were reviewed. Then, various distances from source stopping positions to the bony structures surrounding nasopharynx cavity were measured on the X-ray images that were used as reference for positioning the virtual applicators in CT slices. The sum of calculated dose distributions from 3DCRT and IBT plans were then used for comparison with IMRT plans.

In paper III, both SIB-IMRT and SIB-IMPT plans were prepared for each patient. Dose prescriptions in cobalt Gray equivalent (Gy_E) to GTV-T, PTV-TN and PTV-N were 72.6 Gy_E, 66 Gy_E, and 52.8 Gy_E, respectively, to be delivered in 33 fractions, five days a week. In dose prescriptions to the target volumes and OARs, an RBE of 1.1 to Co^{60} was assumed for the proton beams. The prescribed doses were normalized to the median dose of the target volumes according to the local guidelines at DKFZ. For preparation of IMRT and IMPT plans, the research version of the inverse treatment planning system KonRad (DKFZ) integrated into the VIRTUOS planning system was used. Optimisations of the plans were based on the same principles as described earlier.

In IMRT plans, nine coplanar, equally spaced, 6 MV photon beams were used. The optimized intensity profile for each beam was used to simulate a step-and-shoot delivery technique with a Siemens linear accelerator equipped with MLC. For definition of the fluence map, five non-zero intensity levels were chosen. On average, 132 segments were used for each IMRT plan.

In IMPT plans, three coplanar proton beams (0º, 45º, 315º or 0º, 60º, 300º) simulating 3D spot-scanning technique were used. The lateral separation and depth modulation of proton pencil beams were 5 and 3 mm, respectively. The initial Full Width at Half Maximum of the proton pencil beams at the patient surface was set to 6 mm. On average, 24,734 spots (range; 15,812 – 39,156) were used for each beam. During the inverse treatment planning, optimization of the relative

weights of the individual proton pencil beams was performed simultaneously for all the beams using various pencil beam energies of 160-200 MeV.

In both papers, a dose homogeneity of -5% to +7% and at least 95% coverage of the target by the 95% isodose of the prescribed dose were aimed. However, this goal was not met in complex cases primarily due to the location of critical OARs in vicinity of the high dose targets (GTV-T/PTV-T and PTV-TN). The dose/dose-volume constraints for OARs in both papers were based on the Radiation Therapy Oncology Group recommendations (88) and our institutional guidelines for IMRT of NPC patients (Table 7). However, after evaluation of IMRT results from paper II, we decided to use more stringent dose constraints for some OARs in the third paper III. In the actual optimizations of IMRT and IMPT plans, sometimes lower dose constraints for OARs had to be used in order to comply with the dose/dose volume constraints presented in table 7.

Table 7. Dose constraints for OARs in paper II & III.

Organ	3DCRT+IBT vs. IMRT (Paper II)	IMRT vs. IMPT (Paper III)
Spinal cord (Dmax)	≤ 50 Gy	≤ 50 Gy_E
Brainstem (Dmax)	≤ 60 Gy	≤ 60 Gy_E
Optic chiasm & nerves (Dmax)	≤ 54 Gy	≤ 54 Gy_E
Temporal lobe (Dmax)	≤ 65 Gy	≤ 65 Gy_E
Mandible/TM joints (Dmean) Eye (Dmean)	≤ 75 Gy < 35 Gy	≤ 60 Gy_E < 25 Gy_E
Inner ear (Dmean)	< 50 Gy	< 45 Gy_E
Middle-external ear (Dmean)	< 50 Gy	< 40 Gy_E
Parotid (Dmean)	< 26 Gy	< 26 Gy_E
Larynx-esophagus (Dmean)	< 45 Gy	< 30 Gy_E
Thyroid gland (Dmean)	As low as possible	< 30 Gy_E

*Dmax is the maximum dose in a single voxel. TM = temporomandibular. Gy = Gy_E.

Quantitative comparison of the plans:

The quantitative comparison of the plans for target volumes in papers II and III was performed using Dmean, D1 (Dmax), D99 (Dmin), V95, V105, CI (conformity index defined as the ratio

between the absolute values for V95 of the body and the V95 of the target). Since application of IBT by itself introduced inhomogeneous dose distributions in the combined plans, we did not use any inhomogeneity index for plan evaluations in paper II. In paper III, inhomogeneity coefficient (IC) was defined as Dmax-Dmin/Dmin. In this study, all parameters for PTV-TN and PTV-N were calculated for inclusive volumes of the targets due to the limitations of the VIRTUOS planning system in calculating exclusive volumes.

Radiobiological comparison of the plans was performed only in paper II by using TCP, NTCP, and EUD parameters. The extracted differential DVHs from the plans were used for estimation of TCP and NTCP, using the Bioplan software package (72). TCP of primary tumour was estimated using the volume of GTV-T and differential DVH of PTV-T. The rationale for selecting DVH of PTV-T instead of GTV-T was the expected movement of GTV-T in the volume of PTV-T during the external RT, due to patient movements and setup errors. The assumptions used for TCP calculations were: $\alpha = 0.4$ Gy^{-1}, $\sigma = 0.09$ Gy^{-1}, $\alpha/\beta = 10$ Gy, and homogenous clonogenic cell density of 10^7 cells per cm^3. Two parameters, TCP1 and TCP2, were used to denote estimates uncorrected and corrected for the accelerated repopulation of the tumour cells after 28 days and dose loss of 0.6 Gy/day (89). Compared with paper I, we chose to increase the daily compensating dose for the accelerated repopulation of tumour cells in paper II. In paper I, we assumed an average compensating dose of 0.5 Gy/day for a population of NPC patients with variable WHO type histologies. This value was adapted from two previous reports on combined external irradiation and IBT in NPC patients (20, 84). In the biological model that we used for TCP calculations in paper II, tumour histology could not be incorporated as an independent variable. Therefore, we adapted a compensating dose of 0.6 Gy/day as it has been suggested for H & N cancers in general (89). For EUD calculations of PTV-T, SF2 value of 0.38 was computed based on the assumed biological parameters and formula below.

$$SFd = \exp(-\alpha d - \beta d^2)$$

For OAR comparisons, we used Dmax (single voxel) and Dmean for organs with mainly parallel structures, and Dmax (single voxel) for those with mainly serial structures. The LKB model (74, 75) was used for prediction of NTCP values using parameters shown in table 8.

Table 8. Parameter sets for calculation of NTCP of organs at risk according to the LKB-model.

Organs at risk	TD50 (Gy)	n	m	Endpoint
Brain	60	0.25	0.15	Necrosis/infarction (77)
Ear middle/external	40	0.01	0.15	Acute serous otitis (77)
Ear middle/external	65	0.01	0.095	Chronic serous otitis (77)
Larynx	70	0.08	0.17	Laryngeal edema (77)
Parotid gland	28.4	1.00	0.18	Xerostomia (79)
TM joint	72	0.07	0.1	Marked trismus (77)

TM = temporomandibular.

Statistical analysis

In papers I and IV, the local (LRFS), regional (RRFS), locoregional (LRRFS), and distant (DRFS) relapse-free survival, as well as the disease-free (DFS), progression-free (PFS), and OS rates were calculated using the Kaplan-Meier method and the computed curves were compared using Log-rank test. All survival events were measured from the first day of treatment (CHT or RT). In computing the survival curves of LRFS, RRFS, LRRFS, DRFS, and DFS, patients were censored only in cases of lost to follow-up, last follow-up, and death. Locally persistent tumours were also included in computing the LRFS, LRRFS, DFS, and PFS rates and the failure dates were set at 3 months after the conclusion of the treatments. In DFS, failure at any site was defined as an event. In PFS, failures at any site or death of any cause were labled as events. The impact of prognostic factors on survival probabilities was estimated using univariate and multivariate analysis according to log-rank tests and stepwise Cox proportional hazard models. Fisher´s exact tests and Spearman´s rank correlation test were used for evaluation of the association between two categorical and two continuous variables, respectively. In paper II and III, Wilcoxon signed ranks test was used for statistical inference of paired samples. All tests were two-sided and conducted at 5% significance level.

RESULTS AND DISCUSSION

Paper I:

The purpose of this study was to investigate the clinical manifestations and treatment outcomes in a cohort of Swedish NPC patients and to identify the key aspects for future improvements.

Out of 52 NPC patients initially enrolled in the study, 71% of the patients had stages III-IV at presentation. Majority of the patients (87%) had tumours with WHO type II-III histology. The most common clinical manifestations at diagnosis were neck mass (54%), auditory disturbances (50%), head or neck pain (44%), nasal obstruction and discharge (42% and 31%), weight loss (21%), and cranial nerve involvement (19%).

Survival analysis for 49 nondisseminated patients revealed 5-year DFS, PFS, and OS rates of 61%, 48%, and 55% respectively (Figure 12). The 5-year LRFS, RRFS, and DRFS rates were 70%, 92%, and 77% (Figure 12). Univariate analysis revealed the significant influence of T stage on local tumour control (HR 1.53, 95% CI=1.02-2.29), and tumour stage on distant tumor control rates (HR 3.11, 95% CI=1.29-7.48). The 5-year LRFS rate in T3-T4 tumours was significantly lower than T1-T2 tumours (51% vs. 85%, $p<0.05$). All distant failures were correlated with Stage IVa-b disease. The median times to local and distant failures were 42.7 and 17.6 months, respectively. The results of multivariate analysis demonstrated that WHO type I histology, absorbed dose expressed in $EQD2_{10\text{-}XRT/BT}$ below 66 Gy, and long-standing symptoms before diagnosis had significantly negative impact on LRFS rates. Increasing tumour stage and cranial nerve involvement were significantly associated with inferior DRFS rates. Tumour response within six months after treatment was a significant prognosticator of DFS and PFS rates both when starting point for the analysis was set at the first day of treatment or six months after conclusion of the treatment.

Evaluation of CHT-related toxicities revealed that these were generally mild. Non-hematological side effects of grade III-IV were observed in five patients out 36 who had received CHT. Acute side effects of RT included mucositis (grade II-III) which developed in all patients. As expected, HART was associated with earlier induction of maximum mucositis compared with CRT (median time 17 vs. 35 days). The most common late side effect of irradiation was xerostomia. Grade II and III chronic xerostomia was observed in 80% of the patients. Subjective hearing deterioration was observed in 64% of the patients and 44% were in need of hearing aid. Grade II-III otitis media or externa and grade II hypothyroidism were observed in 66% and 24% of the patients, respectively.

Asymptomatic and symptomatic temporal lobe necroses were observed in 8% and 4% of the patients, respectively. The median time to diagnosis of this side effect was 3.9 years (range 2.1-5.8 years). Other common side effects included trismus, tinnitus, and nasal/nasopharyngeal adhesions.

The clinical manifestations of NPC in our patients have been in line with historical reports (1, 31) including the rate of locoregionally advanced disease (stage III-IV) which was reported in 50% to 90% of NPC patients by previous studies (1, 9, 29, 47, 84). The 13% presence of WHO type I tumours in our study is also expected being a nonendemic patient material. This histology type was reported in 5% and 19% of the NPC patients included in two recent studies from nonendemic regions (35, 90). Although some surveys have demonstrated correlation of nonlymphoepithelioma tumours with worse LRFS and disease-specific survival rates (31, 91), this has not been confirmed by all studies (90). The limited number of the patients included in these studies and the inter-institutional variations in treatment strategies can result in such controversies.

The tumour control and OS rates for our NPC population are seemingly closer to the reports from studies which used radical 2DRT only (1, 31). This observation is somewhat surprising since majority of our patients (71%) had received CHT and all irradiations were delivered with 3DCRT. However, the age of our population was relatively higher compared with many other reports on NPC patients (median 60 vs. 43-49 years) (9, 10, 35, 68). Subsequent compromised constitutional status of the patients by itself or through necessitating treatment modifications could be among factors affecting the outcomes. The results of published reports on the benefits of neoadjuvant and concomitant CHT with RT on LRRFS and DRFS rates in locoregionally advanced NPC (5) was not confirmed for the subgroup of our patients who received CHT with curative intension. The small magnitude of the study population, modifications in dose, timing, or number of delivered cycles in almost half of the patients, and the fact that concomitant cisplatin-based CHT was not delivered to any of our patients are among factors obscuring the expected benefits. Nevertheless, the overall 3 to 5-year DRFS rates of 77-80% in our study is comparable with most other studies including those using IMRT (2, 9, 90). The 5-year LRFS rate of 70% in our NPC patients (51% for T3-T4 tumors) is however disappointingly low which in part is explained by presentation of WHO type I tumours. Baseline diagnostic MRI was lacking in three out of twelve patients with local failure including two patients with T4 disease. Inadequate pre-therapeutic radiologic data or limitations in adequate coverage of the primary tumour by 3DCRT in some of these patients could

be contributing factors to local failure. Detailed study of the original treatment plans is surely of interest to identify the exact localization of the failures with respect to dose distribution. In this study, the median delivered dose by external RT was 63 Gy ($EQD2_{10\text{-}XRT}$) which radiobiologically is relatively low compared to other series (9, 10, 68). It is conceivable that the benefit of dose escalation by brachytherapy in locally advanced tumours was offset by inadequate target coverage due to the rapid dose fall-off from the radioactive sources, although the median delivered dose expressed in $EQD2_{10\text{-}XRT/BT}$ was 68.4 Gy.

Our conclusion is that despite using 3DCRT + IBT for our NPC patients, local and distant failures in locoregionally advanced tumors and the long-term complications of irradiation remain as the main objectives for further improvements.

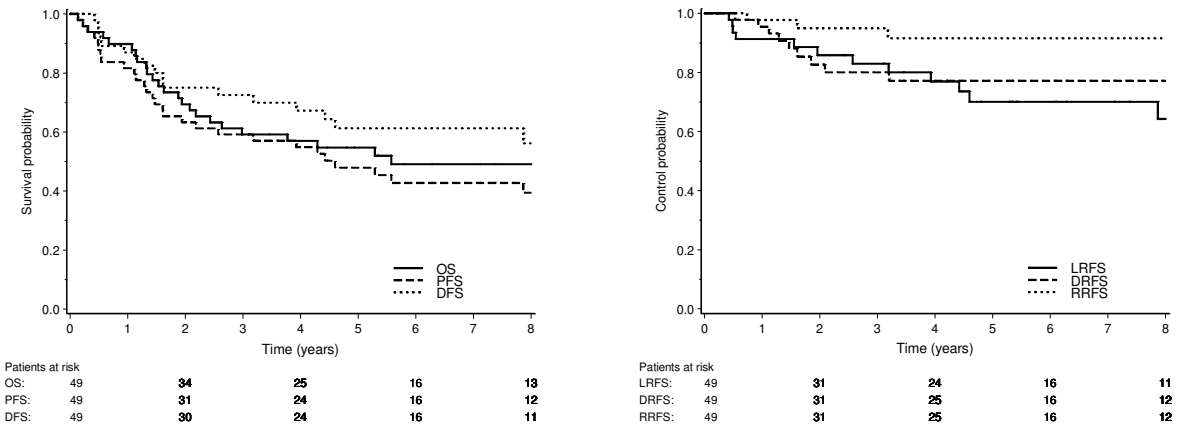

Figure 12. Kaplan-Meier curves for LRFS, DRFS, and RRFS probabilities (right) and DFS, PFS, and OS probabilities (left) in 49 NPC patients.

Paper II:

Based on the treatment outcomes in the first paper, we aimed to study whether improving RT techniques would potentially be beneficial for NPC patients in terms of local tumour control and RT-related side effects. Thus, comparing of IMRT with 3DCRT+IBT through a treatment planning study was performed. The average of quantitative parameters for target volumes in eight enrolled NPC patients are listed in the table 9.

Table 9. Mean dose-volume and TCP data for target volumes in eight NPC patients.

Parameter	SIB-IMRT		3D-CRT + IBT		
	Mean	1 SD	Mean	1 SD	*p*-value
GTV					
D_{min} (Gy)	67.9	5.6	64.2	4.7	0.016
D_{max} (Gy)	74.4	0.9	86.1	8.1	0.008
D_{mean} (Gy)	72.9	0.7	72.2	2.2	0.313
V95 (%)	96	6	81	18	0.016
V105 (%)	0.08	0.25	17	13	0.008
TCP1 (%)	98	1.8	95.8	3.6	0.016
TCP2 (%)	94.3	4.1	89.9	7.3	0.016
PTV-T					
D_{min} (Gy)	63.7	6.3	59.5	6.0	0.008
D_{max} (Gy)	74.3	0.8	100.3	12.9	0.008
D_{mean} (Gy)	72.2	0.8	72.3	2.4	0.945
V95 (%)	93	7	72	17	0.008
V105 (%)	0.05	0.13	21	12.8	0.008
CI	1.8	0.3	5.4	3.3	0.008
EUD (Gy)	67.0	4.0	63.7	5.2	0.016
PTV-TN					
D_{min} (Gy)	56.4	2.6	50.1	5.3	0.016
D_{max} (Gy)	72.1	0.5	94.4	17	0.008
D_{mean} (Gy)	66	0.3	68.1	3.7	0.031
V95 (%)	91	2.3	87	5	0.148
V105 (%)	10	3	26	20	0.016
CI	1.1	0.05	2.0	0.7	0.008
PTV-N					
D_{min} (Gy)	45.4	1.1	37.2	2.3	0.008
D_{max} (Gy)	64.8	1.6	72.4	5.3	0.008
D_{mean} (Gy)	53.9	0.7	53.2	3.2	0.516
V95 (%)	91	2	92	3	0.211
V105 (%)	23	10	52	20	0.008
CI	1.5	0.2	1.96	0.2	0.008

CI = Conformity index, EUD = Equivalent uniform dose, TCP1/2 = Tumour control probability uncorrected/corrected for tumour repopulation in 17 days, SD = standard deviation.

The presented results demonstrate that despite the modest dose escalation to PTV-T in IMRT plans, tumour coverage and conformity of the plans remained superior compared with combined plans. These were reflected in the average V95 values ranged between 91% to 96% for all target volumes in IMRT compared with corresponding range of 72% to 92% in the combined plans. The

worst V95 values for GTV-T were 83% and 55% in IMRT and combined plans, respectively. These values were observed in one T4 patient with intracranial tumour extension in which tumour coverage was compromized in both techniques due to the dose constraints of surrounding neural tissues. As the consequence of better tumour coverage and slight dose escalation, values for TCP1 (ranges 95.1-99.8% vs. 89.5-99.9%) and TCP2 (ranges 88.2-98.8% vs. 77.7-99.1%) of GTV-T, and EUD of PTV-T (ranges 61.9-71.2 Gy vs. 57.2-71.8 Gy) were also significantly improved in IMRT plans.

The concept of conformal avoidance for OARs, was also better achieved in IMRT plans. The averaged Dmax for most of serial OARs was significantly lower in IMRT plans. Moreover, IMRT plans generated significantly lower Dmean for TM joints, middle/external ears, and parotid glands, with consequently lower NTCP values for these OARs (Table 10). For optic chiasm, pituitary gland, inner ears, and larynx, IMRT plans generated higher doses in terms of Dmax or Dmean.

When results were separated for T1-T2 versus T3-T4 tumours and compared between the two techniques, the maximum expected gain in TCP of GTV-T with IMRT plans was 6.7% for T_3-T_4 and 2% for T_1-T_2 tumours. The gain of EUD for PTV-T was about 3 Gy in both T groups. OARs located near GTV-T, such as the temporal lobes, TM joints, and middle-outer ears, were spared better in T_1-T_2 tumours, resulting in lower averaged NTCP values.

Previous comparative treatment planning studies between IMRT and 3DCRT for various stages of NPC have demonstrated the potentials of the former technique in improving tumour coverage, dose homogeneity, dose escalation beyond 70 Gy, and simultaneous dose reduction to OARs such as brainstem, spinal cord, temporal lobes, TM joints, and parotid glands (92, 93). Despite the frequent application of IBT especially in early stages of NPC, none of these comparative studies has addressed the impact of this modality in local tumour control of the disease. Our results revealed a very modest value of IMRT in improving already high rate of local tumour control rates accomplished by 3DCRT+IBT in T1-T2 NPC tumours. IMRT seemed to be more beneficial in locally advanced disease in which increased risk of marginal miss with 3DCRT is unlikely to be remedied by dose escalations of IBT, a technique that by itself is insufficient for adequate dose distribution in large tumour volumes. Although comparison of the results in paper I and II concerning the probability of local tumour control indicate that optimization of 3DCRT plans per se can be beneficial, dose escalation and simultaneous dose reduction in several OARs with 3DCRT in complex cases such as NPC can result in highly inhomogeneous plans (92). Clinical

reports of IMRT in T1-T4 NPC delivering doses of 66-76 Gy have shown 2 to 4-year local/locoregional control rates of 88-97% (2, 3, 44-46) which is in line with the predictions of this paper. Most of these studies reported simultaneous dose reduction to critical neural structures, parotids, TM joints, and ears. In these series, dose reductions for parotids did not seem to have significant impact on acute xerostomia. However, with average Dmean or D50 of about 35 Gy to parotids (2, 45) no grade III long-term xerostomia was observed in any of the enrolled patients. Our IMRT plans achieved an average Dmean of 40 Gy in parotids. The sparing of these glands is highly dependent on dose prescription to the nearby target volumes and their overlapping outlining with parotids. We included deep lobes of parotids in PTV-TNs or PTV-Ns when delineating these targets which explains the higher observed dose and poorer NTCP values for the glands in our study.

It must be emphasized that the absolute values presented for the biological endpoints in this study are prone to error due to the uncertainties concerning the reliability of the background biological parameters and limitations of the applied TCP and NTCP models to incorporate the biological effects of other variables such as histology and CHT. Despite these limitations, the relative difference of the values for biological endpoints between the two studied RT techniques remains reliable.

Based on the results of this paper and previous reports, we conclude that IMRT has a promising role in improving the therapeutic ratio for NPC patients. However, there are few important notions that should be considered. In locally advanced tumours extending to and in neural tissues, tumour coverage with escalated dose prescriptions in IMRT may not be optimal due to the dose constraints of radiosensitive neural tissues. When numerous OARs are chosen for protection, the potential of IMRT in conformal avoidance of all of these may not be unequivocal as a trade-off for optimal tumour coverage and sparing of vital structures. The concept of SIB technique delivering doses above 2 Gy to GTV-T or PTV-T may result in unexpected side effects due to the sensitivity of the embedded normal tissues to fractionation doses. It is therefore important to evaluate the type and volume of the normal tissues that are located within the high dose targets before a decision is made on dose and fractions in SIB-IMRT. As one of the constraints in paper II, fraction sizes above 2 Gy was avoided in critical structures.

One of the major concerns with IMRT is the increased risk of second malignancies primarily because of the expansion of low dose volumes and secondarily because of the increased radiation

scatter from the linear accelerators as a result of increments in monitor units that are needed per target dose when IMRT is delivered. Comparative treatment planning studies between IMRT and 3DCRT for brain tumours (94) have failed to show any significant difference between the two techniques for the volumes exposed to intermediate (10-30 Gy) or very low doses (< 5 Gy). Similar conclusion has been made for the volumes of intermediate doses (10-20 Gy) in H & N cancer by Cozzia et al (95). However, the spatial distributions of low to intermediate doses are usually different for IMRT and 3DCRT plans which merits further investigations with respect to induction of second malignancies in different tissues. Our IMRT plans resulted in significant increase of volumes of 0.66 Gy to 19.8 Gy isodoses (V1 to V30 of the body). On average, these volumes were expanded by 30% to 44% in IMRT plans compared to 3DCRT + IBT plans. These increments of low to intermediate dose volumes could be the result of SIB technique and a higher prescribed dose to PTV-T in IMRT plans and this must be considered when SIB-IMRT is chosen to replace the boosting role of brachytheapy in NPC patients. Based on increments in monitor units, Verellen et al. (96) have estimated eight fold increase in risk of second malignancies when 70 Gy with 6 MV photon beams were delivered with IMRT technique to H & N cancer patients. However, it has also been suggested that the dose contribution to the patients from radiation scattering and its importance in induction of second malignancies in IMRT is only of second order compared with the effect of low to intermediate isodose expansions (95, 97).

Finally, accurate definition of target volumes before and during RT with high-precision conformal techniques such as IMRT is critical. While small errors in the delineation of a tumour may be balanced when the prescribed isodose covers a larger shell than PTV in 2DRT or 3DCRT (less conformal plans), the same errors may have detrimental effects in IMRT. Moreover, changes in tumour shape or patient geometry during the course of IMRT may blur the dose distribution significantly. Hence, the ultimate goal of IMRT in increasing therapeutic ratio is also dependent on optimal diagnostic imaging, standardized definition of target volumes, and dynamic monitoring of tumour and patient geometries during the course of treatment by using image-guided RT.

Table 10. Mean dose-volume and NTCP data for organs at risk in eight NPC patients.

Parameter	SIMT-IMRT		3D-CRT + IBT		
	Mean	1 SD	Mean	1 SD	*p*-value
TM joints					
D_{mean} (Gy)	45.4	7.5	62.3	3.8	<0.001
NTCP-trismus (%)	2	3.6	11	6.1	<0.001
Inner ears					
D_{mean} (Gy)	40.3	8	34.5	11.8	0.024
Middle and external ears					
D_{mean} (Gy)	33.7	6	47.5	7.6	<0.001
NTCP-acute otitis (%)	74.4	28.7	98.6	5.5	<0.001
NTCP-chronic otitis (%)	5.6	10.4	27.5	16	<0.001
Parotid glands					
D_{mean} (Gy)	40.2	8.5	61.8	4.6	<0.001
NTCP-xerostomia (%)	86.5	26.6	100	0	0.001

NTCP = Normal tissue complication probability, TM = temporomandibular joint, SD = standard deviation.

Paper III:

This study was constructed to investigate the clinical potentials of IMPT compared with IMRT in NPC.

The average values extracted for Dmean of the target volumes were almost the same in IMRT and IMPT plans and both techniques were equal in terms of dose homogeneity in PTV-TN and PTV-N. Surprisingly, average minimum dose (D99) for PTV-TN was significantly lower in IMPT plans by 2.8 Gy_E. In contrast to previous reports (59, 61, 62), IMPT plans were significantly more conformal for all target volumes and more homogeneous in GTV-T. The mean V95 for all targets ranged between 93.3% to 97.6% in IMPT versus 87.7% to 93% in IMRT plans. The worse V95 values for GTV-T in IMPT and IMRT plans were 91% and 81%, respectively, and they were observed in the same patient with T4 tumour as described in paper II (Figure 13). In this particular case, the dose constraints for temporal lobes at both sides of the tumour, brainstem at behind, and optic chiasm in front gave less degree of freedom in nine-beam IMRT for coverage of GTV-T with the prescribed dose. This problem was less pronounced in the IMPT plan since 3D modulation of Bragg peaks could recover some of the lost degrees of freedom even though only three fields were used. Admittedly, neither non-coplanar beam orientations nor fluence maps more than five levels were tested in IMRT plans, two approaches which potentially might have improved the conformity of the IMRT plans to some extent. On the other hand, non-coplanar beam orientations or smaller spot size in IMPT plans were not tested either.

In agreement with previous reports, our IMPT plans reduced the integral dose (expressed as average Dmean) in many OARs such as the auditory apparatus, temporal lobes, TM joints, larynx/esophagus, and thyroid gland by a factor of 2 to 3. However, for locally advanced tumours, IMPT plans had as much difficulty as IMRT plans in lowering the Dmax to OARs located in the vicinity of the GTV-T covered by the high isodoses. In some of patients, individual Dmax values for the inner and middle/external ears and TM joints were in fact somewhat higher in IMPT plans. For the spinal cord, the averaged Dmax was halved by IMPT plans. The dose to non-specific normal tissues was measured by calculating V0.5 to V50 of the body corresponding to the volumes of the 0.33 Gy_E to 33 Gy_E isodoses. On average, IMRT plans resulted in 1.78 to 2.66-fold increments in these volumes and highest increments was observed for smallest volumes.

Reduction of the integral doses to non-specific normal tissues and OARs below their proposed dose constraints with IMPT in primary treatment of NPC is potentially advantageous in four

groups of patients. These are patients requiring further dose escalation within GTV-T (boost within the boost volume), patients at high risk of local recurrence and thereby re-irradiation, patients at high risk of distant failure for whom concurrent CHT is frequently applied, and paediatric patients for whom tumour failure, increased therapy-induced side effects and risk of second malignancies after RT are all to be considered. In a study of IMRT concurrent with CHT in five paediatric NPC patients, Louis et al. (98) reported remarkable high incidence rate of RT-related grade II-III toxicities in a variety of structures. The increased risk of second malignancies in low-dose volumes of irradiation has been demonstrated by Karlsson et al. (99), reporting a mean intracranial dose of 0.31 Gy_E in Swedish infants who were irradiated for skin hemangioma and later developed intracranial tumours.

Although results of this paper indicate that IMPT can be considered as state of the art RT technique for NPC patients in future, it is imperative to acknowledge that treatment planning and delivery of IMPT for these patients may face some radiobiological pitfalls. As it was described earlier, the rising RBE at distal edge of SOBP of proton beams when high dose target volumes are surrounded by neural tissues is one concerning issue. However, this might be a less problem in IMPT when several beams from different directions are used. It has been demonstrated that proton plans can be radiobiologically optimized by computerized 3D RBE modulation of the beams using dose, LET, and tissue-specific parameters derived from linear-quadratic models (100, 101). The major obstacle in clinical application of such biological optimizations is the reliability and availability of the applied biological parameters. Until these issues are resolved, 3D LET calculations of the proton beam treatment plans can be a useful tool for identification of the "critical zones" (102).

Most 3D proton beam treatment planning systems are based on pencil beam algorithms with path-length scaling according to number of Hounsfield units in the CT data sets. In treatment planning for NPC cases, uncertainties in the Bragg peak positioning can arise because of possible errors in the conversion from CT numbers to stopping power of proton pencil beams (range errors) related to the complex air-bone interfaces in the nasopharyngeal region (103). In that sense, the Monte Carlo based treatment planning algorithms may model the complex geometries involved in IMPT of NPC patients more properly (104). Another issue for proton therapy is the range shifting of the proton beams during the course of RT as a result of changes in tissue heterogeneities due to such factors as shrinkage of the tumour mass or weight loss. As in IMRT, image-guided RT during the

course of proton therapy can be useful for detecting and correcting daily deviations in the target position and modifying the treatment plans should there be significant changes in the tumour or patient geometries. This can be accomplished by using in-room CTs like linac attached x-ray systems, CT scanner on rails, or functional treatment verification imaging based on the reconstruction of PET signals derived from the nuclear interactions in the trajectory of proton beams (105).

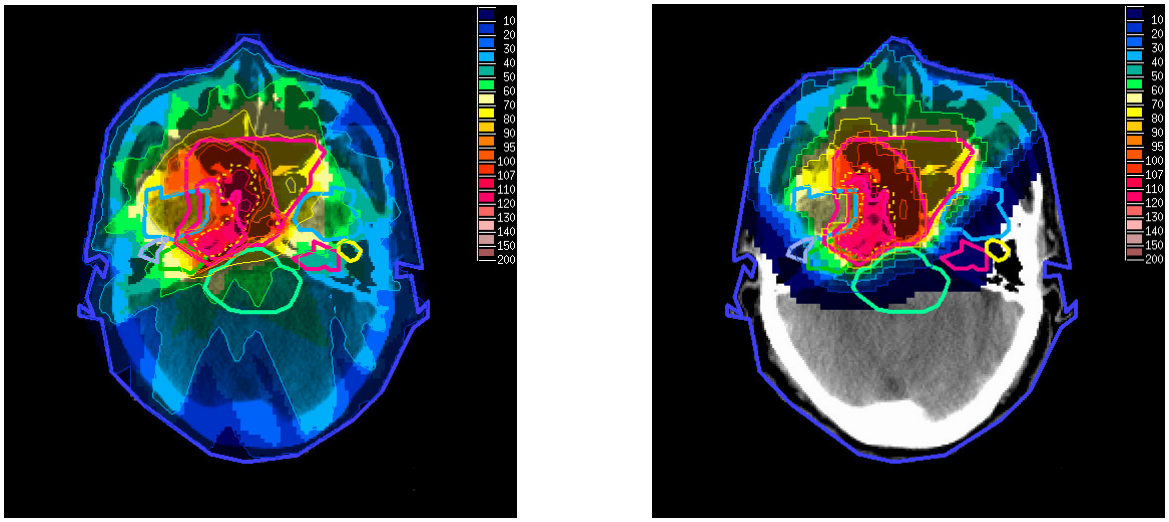

Figure 13. Comparison of isodose distribution between IMPT (right) and IMRT (left) in a T4N1M0 NPC patient. Dotted lines denote 95% isodose of the prescribed dose to GTV-T.

Paper IV:

This paper describes the expression patterns and clinical relevances of LMP1, Ki-67, cyclin-B1, and EGFR in a nonendemic NPC material.

Expression of LMP1 was apparent in 33% of the patients and majority of them were ≤ 50 years. Advanced nodal (N2-N3) and tumour (III-IV) stages were significantly ($P < 0.05$) more presented in LMP1-positive (93% and 100%) than in LMP1-negative (43% and 60%) patients. WHO type III histology was present in 93% of LMP1-positive patients ($p = 0.1$). Although statistically not significant, this correlation reflected the strong association between WHO type III NPC and EBV even in a nonendemic region. Significant correlations between LMP1 expression and younger age and nodal metastasis in NPC patients have been reported in previous studies (106-108). In a survey of 74 WHO type III NPC patients, Hu et al. (22) showed that positive expression of LMP1 was correlated with advanced T and N stages at diagnosis, but that the tumours were less prone to relapse compared with LMP1-negative lesions. In another study of 198 NPC patients who had received radical RT, Yip et al. (14) demonstrated that the presence of EBV-encoded RNA in tumour tissues was significantly correlated with superior 5-year DFS (62% vs. 43%) and OS (80% vs. 56%) rates compared with negative cases. However, there was no significant difference in the 10-year DFS rate between the two group (54% vs. 43%), implying that there is a risk of relapse in EBV-positive NPC patients even several years after primary treatment. Although our results failed to show any significant impact of LMP1 expression on treatment outcomes, they indicated that latent EBV infection may play an important role in oncogenesis of NPC in younger patients or in invasiveness of the cancer also in nonendemic regions.

In this material, all specimens displayed immunoreactivity for Ki-67 and cyclin-B1. The median LI indices for the two markers were 57.8% and 15.8%, respectively. Overexpression of cyclin-B1 was more frequent in patients with N2-N3 than in patients with N0-N1 tumours (67% vs. 35%; $p = 0.08$). No significant correlation between overexpression of Ki-67 or cyclin-B1 and clinical outcomes was found which at least confirms the previous reports for Ki-67 (109, 110).

EGFR expression was observed in 95% of the cases. The extent of expression was < 50% in nine and ≥50% in 35 patients. There were no significant correlations between extent of EGFR expression and patient/tumour variables or any of survival endpoints. However, 93% of the

patients who had tumour failure at any site showed EGFR overexpression (≥ 50%). The intensity of EGFR staining showed significant correlation with all survival endpoints except for DRFS. The estimated 5-year control rates for LRFS, LRRFS, DFS, and OS in patients with staining intensity 0-II versus III were 94%, 94%, 84%, and 77% vs. 49%, 49%, 46%, and 50%, respectively. The impact of staining intensity on survival endpoints was also demonstrated by using MLI scores. The univariate analysis revealed that with a cutoff point at 170, MLI scores ≤ 170 (stronger intensity) were significantly correlated with worse LRFS, LRRFS, and OS rates. When MLI scores were used as a continuous variable, their significant impact was only found for LRFS rates. In multivariate analysis, strong EGFR expression measured semi-quantitatively was an independent prognostic factor for OS rates only after exclusion of age.

Epidermal growth factor receptor is frequently overexpressed in non-NPC, H & N cancers and there are indications that EGFR overexpression in these tumours is associated with poor locoregional tumour control and survival rates after RT (111). This receptor is also frequently expressed in NPC patients (73-100%)(21, 23, 109, 112). Two studies of undifferentiated NPC patients have shown that extent of EGFR expression ≥25% or increasing staining intensity were significantly correlated with worse tumour control rates (21, 109). By contrast, two other studies of non-keratinizing adult and pediatric NPC patients (113, 114) could not show any significant correlation between EGFR overexpression and tumour control or survival rates. It is noteworthy that in the last two studies, the scoring system for EGFR expression included both the extent and the intensity of EGFR staining, which may have obscured the individual biological effects of these two phenomena.

In general, results of this study indicate that evaluation of EGFR expression in NPC patients may serve as a simple tool in prediction of treatment outcomes. Although semi-quantitative grading of EGFR staining intensity in tumour cells is a relatively established method, we found somewhat different results when semi-quantitative and computerized quantification of the staining intensities were applied. One of the disadvantages of the semiquantitative evaluation method is its liability to intra- and interobserver variations, especially in nonhomogenously stained specimens. This, together with existing interinstitutional variations in methods used for IHC assays, underlines the necessity of implementing standardized procedures for the detection and evaluation of EGFR expression in NPC patients. Nevertheless, the results of this study confirmed by the other two imply that molecular profiling of NPC patients with respect to EGFR expression may identify a

subgroup of patients with poor prognosis who might benefit from modifications of the conventional treatments. Whether EGFR can actually serve as a therapeutic target in primary treatment of NPC patients with a significant impact on the clinical outcomes remains to be determined by clinical trials.

Future perspectives and general discussions

In recent decades, much experience has been gained in treating NPC patients. In primary treatment, the minimum acceptable dose for radical RT, and the place of CHT for different stages of the tumour are now more clearly defined. Along with improving tumour control and survival rates in NPC patients, more attention is paid to the RT-related side effects and the quality of life of surviving patients. Thus safe sparing of healthy tissues has become one of the main objectives of modern RT techniques when it concerns NPC. New irradiation techniques such as IMRT have shown encouraging results in dose escalation and widening of the therapeutic ratio for NPC patients which may weaken the role of brachytherapy in primary treatment of the disease. In future, proton therapy and especially IMPT may even have a stronger role in reducing the risk of long-term side effects in a broad range of normal tissues in these patients. Although the prospects of new RT techniques are very promising, their implementation and ultimate realization demands rigorous multidisciplinary efforts and economical investments.

Despite the dose escalation possibilities with modern RT techniques and routine application of chemotherapy, a significant number of NPC patients suffer from distant failures, and local relapse still occurs in locally advanced tumours. It is possible that introduction of new CHT agents and optimal sequencing of these with RT may improve the outcomes for NPC patients. However, It is conceivable that if we are aiming for dramatic improvements in the tumour control and survival rates in these patients, strategic interventions should also consider the biology of the tumor. The close association between EBV and WHO type III NPC even in nonendemic regions, may pave the way for introduction of immune therapy, as it has been proposed, with EBV-specific cytotoxic T lymphocytes in EBV-positive tumours (115). The association of high EBV-DNA plasma concentrations prior and after treatment with poorer survival rates (116) may be used as a benchmark for identification of the subgroup of NPC patients who can benefit from immune therapy. Frequent overexpression of EGFR in NPC patients has opened the door for targeted therapy. Combination of anti-EGFR monoclonal antibodies (cetuximab) and carboplatin in EGFR-positive and cisplatin-resistant NPC patients with recurrent or metastatic tumour has shown some clinical benefits (117) indicating that EGFR may serve as a therapeutic target even in primary treatment of the tumour. Overexpression of vascular endothelial growth factor A (VEGF-A) in NPC patients and its association with higher rates of tumour recurrence and lower survival rates has been

recognized (118) and is rationale for RTOG´s phase II trial of combination of anti-VEGF monoclonal antibody (Bevacizumab) with chemoradiotherapy in locoregionally advanced NPC (119). It is likely that in future, more therapeutic molecules will be included in multimodal treatments of NPC patients. Although potentially beneficial for tumour control, these approaches may inevitably increase the rate of adverse toxicities in NPC patients which necessitates introduction of RT modalities with least side effects at risk of aggravation by adjunctive therapy.

Finally, the subject of NPC in nonendemic regions needs to be addressed from a practical point of view. Due to the rarity of the disease in these regions, single institutional performance of randomized clinical trials investigating medical efficacy of novel therapeutic strategies is indeed out of reality. However, multi-institutional or international cooperations can provide possibilities for conducting such trials with patient accrual even from nonendemic regions. Furtheremore, such collaborations are valuable platforms for exchanging experience and standardizing treatment protocols for NPC patients.

CONCLUSIONS

- In early stages of nasopharyngeal carcinoma, delivering of standard absorbed doses with combination of 3DCRT and IBT yields encouraging tumour control rates.

- The treatment outcomes for locoregionally advanced tumours applying the same approach and even with addition of chemotherapy remains unsatisfactory with respect to local and distant tumour control.

- Despite the application of 3DCRT in nasopharyngeal carcinoma, the incidence of adverse radiotherapy-related side effects is high because of numerous normal structures that are affected by irradiation.

- Intensity-modulated radiotherapy provides better conformal coverage of the tumours and conformal avoidance of the normal structures when treating nasopharyngeal carcinoma. However, the potentials of this technique can be limited when numerous radiosensitive structures are to be protected simultaneously.

- In nasopharyngeal carcinoma, intensity-modulated proton therapy provides additional benefits in increasing the therapeutic ratio primarily by reduction of integral dose to non-targeted tissues and secondarily by better tumour coverage in locally advanced tumours.

- Improvement in radiotherapy techniques may not affect the rate of distant-failure in patients with locoregionally advanced nasopharyngeal carcinoma and thereby innovations in the adjunctive therapy of these patients are still needed.

- The correlation of LMP1 with tumour stage and EGFR expression with treatment outcomes in nasopharyngeal carcinoma define a subset of patients that might benefit from novel treatment strategies such as targeted therapy.

ACKNOWLEDGEMENTS

This project was supported by the King Gustav V Jubilee Clinical Cancer Research Foundation in Göteborg.

I wish to express my sincere gratitude to all the people who have supported me to accomplish this thesis and particular thanks to:

Associate professor *Thomas Björk-Eriksson* my supervisor and colleague and head of the department of radiotherapy, for pushing me into the field of research, providing me time and useful connections to work on this project, your mentorship and inspiration, and teaching me not to give up.

Associate professor *Karl-Axel Johansson* my co-supervisor and colleague for your novel ideas, unlimited and comprehensive support, teaching me analytical thinking, and for your patience when I did not understand physics.

Professor *Claes Mercke* my co-supervisor for your encouragement, fruitful discussions, and educational support.

Professor *Ragnar Hultborn,* head of the Department of Oncology, the institute of clinical sciences, for your creative mind and positive attitude, scientific guidance, help, and advising me to choose the path of creation not administration.

Professor emeritus *Arne Wallgren* for your sharp insight, constructive criticisms, and believing in me.

Colleagues at DKFZ, Heidelberg; my co-authors, *Dr. Marc Münter,* professor *Uwe Ölfke, Simeon Nill, and Jan Wilkens* for your tremendous support with the proton project and a great collaboration, professor *Oliver Jäkel* for your support in initiation of the work and scientific contributions, and also *Dr. Alex Jensen & Dr. Florian Sterzing* for your kind friendships.

Professor *Bengt Magnusson & Marie Svensson,* my co-authors, for your help with the study of biomarkers and bringing the subject of pathology back to me.

All the colleagues at Jubileumskliniken for your friendship, solidarity, and sense of humour.

Colleagues at team four and department of radiotherapy especially *Jan Nyman, Hillevi Rylander, Edvard Abel, Hedda Haugen and Christina Goldkuhl* for your support and taking care of my patients during the research period.

Kerstin Thalén & Åse Blennius for your enormous help with all the practicalities and being always in a good mood.

Aldina Pivodic for all the statistical analysis and having patience with my requests and questions.

All the staff at the department of radiotherapy and in- and out-patient departments for your dedicated working styles, cheerful attitudes, and for making the impossible possible in every day.

All the staff at the department of radiophysics especially *Magnus Gustavssov, Sven Hertzman, Niclas Pettersson, Caroline Olsson, and Emma Djärv* for your scientific contributions.

My parents, for your never-ending love, encouragement, wisdom, and support through the years.

My sister, for your love, friendship, support, and all those long laughing conversations.

My brothers, Jane and in-laws for always being there for me despite the distance.

My friends, *Zohreh & Hengameh* for your genuine friendships and understanding.

REFERENCES

1. Yeh SA, Tang Y, Lui CC, et al. Treatment outcomes and late complications of 849 patients with nasopharyngeal carcinoma treated with radiotherapy alone. Int J Radiat Oncol Biol Phys 2005;62:672-679.
2. Lee N, Xia P, Quivey JM, et al. Intensity-modulated radiotherapy in the treatment of nasopharyngeal carcinoma: an update of the UCSF experience. Int J Radiat Oncol Biol Phys 2002;53:12-22.
3. Kam MK, Teo PM, Chau RM, et al. Treatment of nasopharyngeal carcinoma with intensity-modulated radiotherapy: the Hong Kong experience. Int J Radiat Oncol Biol Phys 2004;60:1440-1450.
4. Baujat B, Audry H, Bourhis J, et al. Chemotherapy in locally advanced nasopharyngeal carcinoma: an individual patient data meta-analysis of eight randomized trials and 1753 patients. Int J Radiat Oncol Biol Phys 2006;64:47-56.
5. Langendijk JA, Leemans CR, Buter J, et al. The additional value of chemotherapy to radiotherapy in locally advanced nasopharyngeal carcinoma: a meta-analysis of the published literature. J Clin Oncol 2004;22:4604-4612.
6. Chan AT, Teo PM, Johnson PJ. Nasopharyngeal carcinoma. Ann Oncol 2002;13:1007-1015.
7. Swedish Cancer Registry. Cancer incidence in Sweden 2000-2004. Stockholm: Swedish National Board of Health and Welfare (Socialstyrelsen), Centre for Epidemiology; 2001-2005.
8. Ozyar E, Selek U, Laskar S, et al. Treatment results of 165 pediatric patients with non-metastatic nasopharyngeal carcinoma: a Rare Cancer Network study. Radiother Oncol 2006;81:39-46.
9. Palazzi M, Guzzo M, Tomatis S, et al. Improved outcome of nasopharyngeal carcinoma treated with conventional radiotherapy. Int J Radiat Oncol Biol Phys 2004;60:1451-1458.
10. Teo PM, Leung SF, Chan AT, et al. Final report of a randomized trial on altered-fractionated radiotherapy in nasopharyngeal carcinoma prematurely terminated by significant increase in neurologic complications. Int J Radiat Oncol Biol Phys 2000;48:1311-1322.
11. International histological classification of tumours. Histological typing of upper respiratory tract tumours. Geneva: World Health Organization; 1978. Report No:19.
12. Wei WI, Sham JS. Nasopharyngeal carcinoma. Lancet 2005;365:2041-2054.
13. Kalpoe JS, Dekker PB, van Krieken JH, et al. Role of Epstein-Barr virus DNA measurement in plasma in the clinical management of nasopharyngeal carcinoma in a low risk area. J Clin Pathol 2006;59:537-541.
14. Yip KW, Shi W, Pintilie M, et al. Prognostic significance of the Epstein-Barr virus, p53, Bcl-2, and survivin in nasopharyngeal cancer. Clin Cancer Res 2006;12:5726-5732.
15. Schantz S.P, Harrison LB, Forastiere AA. Nasopharynx. In: Cancer, Principles and Practice of Oncology. Vol 1. 6th ed: Lippincott Williams & Wilkins; 2001. pp. 824-832.
16. Kumar MB, Lu JJ, Loh KS, et al. Tailoring distant metastatic imaging for patients with clinically localized undifferentiated nasopharyngeal carcinoma. Int J Radiat Oncol Biol Phys 2004;58:688-693.
17. Ho JH. Stage classification of nasopharyngeal carcinoma: a review. IARC Sci Publ 1978:99-113.

18. Fleming ID, Cooper JS, Henson DE. American Joint Committee on Cancer manual for staging of cancer. 5th ed. Philadelphia, PA: Lippincott-Raven; 1997.
19. Sobin LH, Fleming ID. TNM Classification of Malignant Tumors, fifth edition (1997). Union Internationale Contre le Cancer and the American Joint Committee on Cancer. Cancer 1997;80:1803-1804.
20. Teo PM, Leung SF, Lee WY, et al. Intracavitary brachytherapy significantly enhances local control of early T-stage nasopharyngeal carcinoma: the existence of a dose-tumor-control relationship above conventional tumoricidal dose. Int J Radiat Oncol Biol Phys 2000;46:445-458.
21. Chua DT, Nicholls JM, Sham JS, et al. Prognostic value of epidermal growth factor receptor expression in patients with advanced stage nasopharyngeal carcinoma treated with induction chemotherapy and radiotherapy. Int J Radiat Oncol Biol Phys 2004;59:11-20.
22. Hu LF, Chen F, Zhen QF, et al. Differences in the growth pattern and clinical course of EBV-LMP1 expressing and non-expressing nasopharyngeal carcinomas. Eur J Cancer 1995;31A:658-660.
23. Zheng X, Hu L, Chen F, et al. Expression of Ki67 antigen, epidermal growth factor receptor and Epstein-Barr virus-encoded latent membrane protein (LMP1) in nasopharyngeal carcinoma. Eur J Cancer B Oral Oncol 1994;30B:290-295.
24. Hassan KA, El-Naggar AK, Soria JC, et al. Clinical significance of cyclin B1 protein expression in squamous cell carcinoma of the tongue. Clin Cancer Res 2001;7:2458-2462.
25. Hassan KA, Ang KK, El-Naggar AK, et al. Cyclin B1 overexpression and resistance to radiotherapy in head and neck squamous cell carcinoma. Cancer Res 2002;62:6414-6417.
26. Al-Sarraf M, LeBlanc M, Giri PG, et al. Chemoradiotherapy versus radiotherapy in patients with advanced nasopharyngeal cancer: phase III randomized Intergroup study 0099. J Clin Oncol 1998;16:1310-1317.
27. Wang CC. Carcinoma of the nasopharynx. In: Radiation therapy for head and neck neoplasms, indications, techniques, and results. Second ed: Year book Medical Publishers, INC.; 1990. pp. 261-283.
28. Huguenin PU, Taussky D, Moe K, et al. Quality of life in patients cured from a carcinoma of the head and neck by radiotherapy: the importance of the target volume. Int J Radiat Oncol Biol Phys 1999;45:47-52.
29. Lee AW, Sze WM, Au JS, et al. Treatment results for nasopharyngeal carcinoma in the modern era: the Hong Kong experience. Int J Radiat Oncol Biol Phys 2005;61:1107-1116.
30. Ho JH. An epidemiologic and clinical study of nasopharyngeal carcinoma. Int J Radiat Oncol Biol Phys 1978;4:182-198.
31. Sanguineti G, Geara FB, Garden AS, et al. Carcinoma of the nasopharynx treated by radiotherapy alone: determinants of local and regional control. Int J Radiat Oncol Biol Phys 1997;37:985-996.
32. ICRU Reports 50/62, Prescribing, Recording, and Reporting Photon Beam Therapy: International Commission on Radiation Units and Measurements, Inc; 1993/1999.
33. Leibel SA, Kutcher GJ, Harrison LB, et al. Improved dose distributions for 3D conformal boost treatments in carcinoma of the nasopharynx. Int J Radiat Oncol Biol Phys 1991;20:823-833.
34. Wolden SL, Zelefsky MJ, Hunt MA, et al. Failure of a 3D conformal boost to improve radiotherapy for nasopharyngeal carcinoma. Int J Radiat Oncol Biol Phys 2001;49:1229-1234.

35. Rischin D, Corry J, Smith J, et al. Excellent Disease control and Survival in Patients With Advanced Nasopharyngeal Cancer Treated With Chemoradiation. Journal of Clinical Oncology 2002;20:1845-1852.
36. Lee AW, Yau TK, Wong DH, et al. Treatment of stage IV(A-B) nasopharyngeal carcinoma by induction-concurrent chemoradiotherapy and accelerated fractionation. Int J Radiat Oncol Biol Phys 2005;63:1331-1338.
37. Lomax A. Intensity modulation methods for proton radiotherapy. Phys Med Biol 1999;44:185-205.
38. Nill S, Bortfeld T, Oelfke U. Inverse planning of intensity modulated proton therapy. Z Med Phys 2004;14:35-40.
39. Lauve A, Morris M, Schmidt-Ullrich R, et al. Simultaneous integrated boost intensity-modulated radiotherapy for locally advanced head-and-neck squamous cell carcinomas: II--clinical results. Int J Radiat Oncol Biol Phys 2004;60:374-387.
40. Fu KK, Pajak TF, Trotti A, et al. A Radiation Therapy Oncology Group (RTOG) phase III randomized study to compare hyperfractionation and two variants of accelerated fractionation to standard fractionation radiotherapy for head and neck squamous cell carcinomas: first report of RTOG 9003. Int J Radiat Oncol Biol Phys 2000;48:7-16.
41. Dogan N, King S, Emami B, et al. Assessment of different IMRT boost delivery methods on target coverage and normal-tissue sparing. Int J Radiat Oncol Biol Phys 2003;57:1480-1491.
42. Studer G, Huguenin PU, Davis JB, et al. IMRT using simultaneously integrated boost (SIB) in head and neck cancer patients. Radiat Oncol 2006;1:7.
43. Lee AW, Foo W, Chappell R, et al. Effect of time, dose, and fractionation on temporal lobe necrosis following radiotherapy for nasopharyngeal carcinoma. Int J Radiat Oncol Biol Phys 1998;40:35-42.
44. Lee S-W, Back G, Yi B, et al. Preliminary results of a phase I/II study of simultaneous modulated accelerated radiotherapy for nondisseminated nasopharyngeal carcinoma. Int J Radiat Oncol Biol Phys 2006;65:152-160.
45. Wolden SL, Chen WC, Pfister DG, et al. Intensity-modulated radiation therapy (IMRT) for nasopharynx cancer: update of the Memorial Sloan-Kettering experience. Int J Radiat Oncol Biol Phys 2006;64:57-62.
46. Kwong DL, Sham JS, Leung LH, et al. Preliminary results of radiation dose escalation for locally advanced nasopharyngeal carcinoma. Int J Radiat Oncol Biol Phys 2006;64:374-381.
47. Kristensen CA, Kjaer-Kristoffersen F, Sapru W, et al. Nasopharyngeal carcinoma. Treatment planning with IMRT and 3D conformal radiotherapy. Acta Oncol 2007;46:214-220.
48. Wilson R. Radiological Use of fast Protons. Radiology 1946:487-491.
49. Bragg W. Studies in radioactivity. London; 1912.
50. Pedroni E. Will we need proton therapy in the future? Europhysics news 2000;31.
51. Schulz-Ertner D, Jakel O, Schlegel W. Radiation therapy with charged particles. Semin Radiat Oncol 2006;16:249-259.
52. Grözinger SO. Particle Beam Application, on the way to optimum dose conformity: Siemens medical solutions; 2005.
53. Oelfke U, Bortfeld T. Intensity modulated radiotherapy with charged particle beams: studies of inverse treatment planning for rotation therapy. Med Phys 2000;27:1246-1257.

54. Weber DC, Rutz HP, Pedroni ES, et al. Results of spot-scanning proton radiation therapy for chordoma and chondrosarcoma of the skull base: the Paul Scherrer Institut experience. Int J Radiat Oncol Biol Phys 2005;63:401-409.
55. Fitzek MM, Linggood RM, Adams J, et al. Combined proton and photon irradiation for craniopharyngioma: long-term results of the early cohort of patients treated at Harvard Cyclotron Laboratory and Massachusetts General Hospital. Int J Radiat Oncol Biol Phys 2006;64:1348-1354.
56. Paganetti H. Significance and implementation of RBE variations in proton beam therapy. Technol Cancer Res Treat 2003;2:413-426.
57. Gerweck LE, Kozin SV. Relative biological effectiveness of proton beams in clinical therapy. Radiother Oncol 1999;50:135-142.
58. Baumert BG, Norton IA, Lomax AJ, et al. Dose conformation of intensity-modulated stereotactic photon beams, proton beams, and intensity-modulated proton beams for intracranial lesions. Int J Radiat Oncol Biol Phys 2004;60:1314-1324.
59. Steneker M, Lomax A, Schneider U. Intensity modulated photon and proton therapy for the treatment of head and neck tumors. Radiother Oncol 2006;80:263-267.
60. Weber DC, Trofimov AV, Delaney TF, et al. A treatment planning comparison of intensity modulated photon and proton therapy for paraspinal sarcomas. Int J Radiat Oncol Biol Phys 2004;58:1596-1606.
61. Miralbell R, Cella L, Weber D, et al. Optimizing radiotherapy of orbital and paraorbital tumors: intensity-modulated X-ray beams vs. intensity-modulated proton beams. Int J Radiat Oncol Biol Phys 2000;47:1111-1119.
62. Lomax AJ, Goitein M, Adams J. Intensity modulation in radiotherapy: photons versus protons in the paranasal sinus. Radiother Oncol 2003;66:11-18.
63. Brown AP, Urie MM, Chisin R, et al. Proton therapy for carcinoma of the nasopharynx: a study in comparative treatment planning. Int J Radiat Oncol Biol Phys 1989;16:1607-1614.
64. Noel G, Boisserie G, Dessard-Diana B, et al. [Comparison with dose-volume histograms of two conformal irradiation techniques used for the treatment of T2N0M0 nasopharyngeal cancer, one with association of photons and protons and another with photons alone]. Cancer Radiother 2002;6:337-348.
65. Lin R, Slater JD, Yonemoto LT, et al. Nasopharyngeal carcinoma: repeat treatment with conformal proton therapy--dose-volume histogram analysis. Radiology 1999;213:489-494.
66. Fang FM, Chiu HC, Kuo WR, et al. Health-related quality of life for nasopharyngeal carcinoma patients with cancer-free survival after treatment. Int J Radiat Oncol Biol Phys 2002;53:959-968.
67. Rades D, Fehlauer F, Sheikh-Sarraf M, et al. Toxicity of two cisplatin-based radiochemotherapy regimens for the treatment of patients with stage III/IV head and neck cancer. Head Neck 2007.
68. Lin JC, Chen KY, Jan JS, et al. Partially hyperfractionated accelerated radiotherapy and concurrent chemotherapy for advanced nasopharyngeal carcinoma. Int J Radiat Oncol Biol Phys 1996;36:1127-1136.
69. Sham JS, Choy D, Wei W, et al. Value of clinical follow-up in local nasopharyngeal carcinoma relapse. Head Neck 1992;14:208-217.
70. Wu Q, Mohan R, Niemierko A, et al. Optimization of intensity-modulated radiotherapy plans based on the equivalent uniform dose. Int J Radiat Oncol Biol Phys 2002;52:224-235.

71. Jackson A, Yorke E. NTCP and TCP For Treatment Planning. In: A practical guide to intensity-modulated radiation therapy. NY: Medical Physics Publishing; 2003. pp. 287-320.
72. Sanchez-Nieto B, Nahum AE. BIOPLAN: software for the biological evaluation of. Radiotherapy treatment plans. Med Dosim 2000;25:71-76.
73. Niemierko A. Reporting and analyzing dose distributions: a concept of equivalent uniform dose. Med Phys 1997;24:103-110.
74. Lyman JT. Complication probability as assessed from dose-volume histograms. Radiat Res Suppl 1985;8:S13-19.
75. Kutcher GJ, Burman C. Calculation of complication probability factors for non-uniform normal tissue irradiation: the effective volume method. Int J Radiat Oncol Biol Phys 1989;16:1623-1630.
76. Burman C, Kutcher GJ, Emami B, et al. Fitting of normal tissue tolerance data to an analytic function. Int J Radiat Oncol Biol Phys 1991;21:123-135.
77. Emami B, Lyman J, Brown A, et al. Tolerance of normal tissue to therapeutic irradiation. Int J Radiat Oncol Biol Phys 1991;21:109-122.
78. Longobardi B, De Martin E, Fiorino C, et al. Comparing 3DCRT and inversely optimized IMRT planning for head and neck cancer: equivalence between step-and-shoot and sliding window techniques. Radiother Oncol 2005;77:148-156.
79. Eisbruch A, Ten Haken RK, Kim HM, et al. Dose, volume, and function relationships in parotid salivary glands following conformal and intensity-modulated irradiation of head and neck cancer. Int J Radiat Oncol Biol Phys 1999;45:577-587.
80. Bourhis J, Overgaard J, Audry H, et al. Hyperfractionated or accelerated radiotherapy in head and neck cancer: a meta-analysis. Lancet 2006;368:843-854.
81. Wang CC. Accelerated Hyperfractionation Radiation Therapy for Carcinoma of the Nasopharynx. Techniques and results. Cancer 1989;63:2461-2467.
82. Horiot JC. [Controlled clinical trials of hyperfractionated and accelerated radiotherapy in otorhinolaryngologic cancers]. Bull Acad Natl Med 1998;182:1247-1260; discussion 1261.
83. Wang CC. Accelerated hyperfractionation radiation therapy for carcinoma of the nasopharynx. Techniques and results. Cancer 1989;63:2461-2467.
84. Levendag PC, Lagerwaard FJ, Noever I, et al. Role of endocavitary brachytherapy with or without chemotherapy in cancer of the nasopharynx. Int J Radiat Oncol Biol Phys 2002;52:755-768.
85. Joiner MC, Bentzen SM. Time-dose relationships: the linear-quadratic approach. In: Steel Go, editor. Basic clinical radiobiology. Third ed. London: Arnold; 2002. pp. 120-133.
86. National Cancer Institute. Common Terminology Criteria For Adverse Events, Version 3.0 (CTCAE v3.0); 2003.
87. LENT-SOMA scales for all anatomic sites. Int J Radiat Oncol Biol Phys 1995;31:1049-1091.
88. Lee N, Kramer A, Xia P. A phase II study of intensity-modulated radiation therapy (IMRT) +/- chemotherapy for nasopharyngeal cancer. Protocol 0225: Radiation Therapy Oncology Group; 2003.
89. Withers HR, Taylor JM, Maciejewski B. The hazard of accelerated tumor clonogen repopulation during radiotherapy. Acta Oncol 1988;27:131-146.

90. Yee D, Hanson J, Lau H, et al. Treatment of nasopharyngeal carcinoma in the modern era: analysis of outcomes and toxicity from a single center in a nonendemic area. Cancer J 2006;12:147-154.
91. Geara FB, Sanguineti G, Tucker SL, et al. Carcinoma of the nasopharynx treated by radiotherapy alone: determinants of distant metastasis and survival. Radiother Oncol 1997;43:53-61.
92. Hunt MA, Zelefsky MJ, Wolden S, et al. Treatment planning and delivery of intensity-modulated radiation therapy for primary nasopharynx cancer. Int J Radiat Oncol Biol Phys 2001;49:623-632.
93. Kam MK, Chau RM, Suen J, et al. Intensity-modulated radiotherapy in nasopharyngeal carcinoma: dosimetric advantage over conventional plans and feasibility of dose escalation. Int J Radiat Oncol Biol Phys 2003;56:145-157.
94. Hermanto U, Frija EK, Lii MJ, et al. Intensity-modulated radiotherapy (IMRT) and conventional three-dimensional conformal radiotherapy for high-grade gliomas: does IMRT increase the integral dose to normal brain? Int J Radiat Oncol Biol Phys 2007;67:1135-1144.
95. Cozzi L, Fogliata A, Bolsi A, et al. Three-dimensional conformal vs. intensity-modulated radiotherapy in head-and-neck cancer patients: comparative analysis of dosimetric and technical parameters. Int J Radiat Oncol Biol Phys 2004;58:617-624.
96. Verellen D, Vanhavere F. Risk assessment of radiation-induced malignancies based on whole-body equivalent dose estimates for IMRT treatment in the head and neck region. Radiother Oncol 1999;53:199-203.
97. Schneider U, Lomax A, Pemler P, et al. The impact of IMRT and proton radiotherapy on secondary cancer incidence. Strahlenther Onkol 2006;182:647-652.
98. Louis CU, Paulino AC, Gottschalk S, et al. A single institution experience with pediatric nasopharyngeal carcinoma: high incidence of toxicity associated with platinum-based chemotherapy plus IMRT. J Pediatr Hematol Oncol 2007;29:500-505.
99. Karlsson P, Holmberg E, Lundell M, et al. Intracranial tumors after exposure to ionizing radiation during infancy: a pooled analysis of two Swedish cohorts of 28,008 infants with skin hemangioma. Radiat Res 1998;150:357-364.
100. Wilkens JJ, Oelfke U. Optimization of radiobiological effects in intensity modulated proton therapy. Med Phys 2005;32:455-465.
101. Tilly N, Johansson J, Isacsson U, et al. The influence of RBE variations in a clinical proton treatment plan for a hypopharynx cancer. Phys Med Biol 2005;50:2765-2777.
102. Wilkens JJ, Oelfke U. Three-dimensional LET calculations for treatment planning of proton therapy. Z Med Phys 2004;14:41-46.
103. Schneider U, Schaffner B, Lomax T, et al. A technique for calculating range spectra of charged particle beams distal to thick inhomogeneities. Med Phys 1998;25:457-463.
104. Paganetti H. Monte Carlo method to study the proton fluence for treatment planning. Med Phys 1998;25:2370-2375.
105. Parodi K, Paganetti H, Shih HA, et al. Patient study of in vivo verification of beam delivery and range, using positron emission tomography and computed tomography imaging after proton therapy. Int J Radiat Oncol Biol Phys 2007;68:920-934.
106. Khabir A, Karray H, Rodriguez S, et al. EBV latent membrane protein 1 abundance correlates with patient age but not with metastatic behavior in north African nasopharyngeal carcinomas. Virol J 2005;2:39.

107. Gondhowiardjo S. Epstein-Barr virus latent membrane protein 1 (EBV-LMP1) and tumor proliferation rate as predictive factors of nasopharyngeal cancer (NPC) radiation response. Gan To Kagaku Ryoho 2000;27 Suppl 2:323-331.
108. Horikawa T, Yoshizaki T, Sheen TS, et al. Association of latent membrane protein 1 and matrix metalloproteinase 9 with metastasis in nasopharyngeal carcinoma. Cancer 2000;89:715-723.
109. Ma BB, Poon TC, To KF, et al. Prognostic significance of tumor angiogenesis, Ki 67, p53 oncoprotein, epidermal growth factor receptor and HER2 receptor protein expression in undifferentiated nasopharyngeal carcinoma--a prospective study. Head Neck 2003;25:864-872.
110. Masuda M, Shinokuma A, Hirakawa N, et al. Expression of bcl-2-, p53, and Ki-67 and outcome of patients with primary nasopharyngeal carcinomas following DNA-damaging treatment. Head Neck 1998;20:640-644.
111. Ang KK, Berkey BA, Tu X, et al. Impact of epidermal growth factor receptor expression on survival and pattern of relapse in patients with advanced head and neck carcinoma. Cancer Res 2002;62:7350-7356.
112. Sheen TS, Huang YT, Chang YL, et al. Epstein-Barr virus-encoded latent membrane protein 1 co-expresses with epidermal growth factor receptor in nasopharyngeal carcinoma. Jpn J Cancer Res 1999;90:1285-1292.
113. Leong JL, Loh KS, Putti TC, et al. Epidermal growth factor receptor in undifferentiated carcinoma of the nasopharynx. Laryngoscope 2004;114:153-157.
114. Fang FM, Li CF, Chien CY, et al. Immunohistochemical expression of epidermal growth factor receptor and cyclooxygenase-2 in pediatric nasopharyngeal carcinomas: no significant correlations with clinicopathological variables and treatment outcomes. Int J Pediatr Otorhinolaryngol 2007;71:447-455.
115. Straathof KC, Bollard CM, Popat U, et al. Treatment of nasopharyngeal carcinoma with Epstein-Barr virus--specific T lymphocytes. Blood 2005;105:1898-1904.
116. Twu CW, Wang WY, Liang WM, et al. Comparison of the prognostic impact of serum anti-EBV antibody and plasma EBV DNA assays in nasopharyngeal carcinoma. Int J Radiat Oncol Biol Phys 2007;67:130-137.
117. Chan AT, Hsu MM, Goh BC, et al. Multicenter, phase II study of cetuximab in combination with carboplatin in patients with recurrent or metastatic nasopharyngeal carcinoma. J Clin Oncol 2005;23:3568-3576.
118. Krishna SM, James S, Balaram P. Expression of VEGF as prognosticator in primary nasopharyngeal cancer and its relation to EBV status. Virus Res 2006;115:85-90.
119. Lee N, Pfister DG, Garden A, et al. A phase II study of concurrent chemoradiotherapy using three-dimensional conformal radiotherapy (3D-CRT) or intensity-modulated radiation therapy (IMRT) + Bevacisumab (BV) for locally or regionally advanced nasopharyngeal cancer. RTOG 0615: Radiation Therapy Oncology Group; 2006.